

DNA 3432F

BLAST SIMULATION WITH BALLOONS CONTAINING DETONABLE GAS

ADB001454

General American Research Division
7449 North Natchez Avenue
Niles, Illinois 60648

11 December 1974

Final Technical Report

CONTRACT No. DNA 001-72-C-0058

Distribution limited to U.S. Government agencies only (Test and Evaluation), 19 July 1974. Other requests for this document must be referred to the Director, Defense Nuclear Agency, Washington, D.C. 20305.

THIS WORK SPONSORED BY THE DEFENSE NUCLEAR AGENCY
UNDER SUBTASK V99QAXNA007-28/37/38.

Prepared for
Director
DEFENSE NUCLEAR AGENCY
Washington, D. C. 20305

UNCLASSIFIED

SECURITY CLASSIFICATION OF THIS PAGE (When Data Entered)

REPORT DOCUMENTATION PAGE		READ INSTRUCTIONS BEFORE COMPLETING FORM
1. REPORT NUMBER DNA 3432F	2. GOVT ACCESSION NO.	3. RECIPIENT'S CATALOG NUMBER
4. TITLE (and Subtitle) BLAST SIMULATION WITH BALLOONS CONTAINING DETONABLE GAS		5. TYPE OF REPORT & PERIOD COVERED Final Technical Report
		6. PERFORMING ORG. REPORT NUMBER 1539-6000
7. AUTHOR(s) Stephen F. Fields and Leif E. Fugelso		8. CONTRACT OR GRANT NUMBER(s) DNA 001-72-C-0058
9. PERFORMING ORGANIZATION NAME AND ADDRESS General American Research Division 7449 North Natchez Avenue Niles, Illinois 60648		10. PROGRAM ELEMENT, PROJECT, TASK AREA & WORK UNIT NUMBERS NWED Subtask V99QAXNA007-28/37/38
11. CONTROLLING OFFICE NAME AND ADDRESS Director Defense Nuclear Agency Washington, D. C. 20305		12. REPORT DATE 11 December 1974
		13. NUMBER OF PAGES 60
14. MONITORING AGENCY NAME & ADDRESS (if different from Controlling Office)		15. SECURITY CLASS (of this report) UNCLASSIFIED
		15a. DECLASSIFICATION/DOWNGRADING SCHEDULE
16. DISTRIBUTION STATEMENT (of this Report) Distribution limited to U. S. Government agencies only (Test and Evaluation), 19 July 1974. Other requests for this document must be referred to the Director, Defense Nuclear Agency, Washington, D. C. 20305.		
17. DISTRIBUTION STATEMENT (of the abstract entered in Block 20, if different from Report)		
18. SUPPLEMENTARY NOTES This work sponsored by the Defense Nuclear Agency under Subtask V99QAXNA007-28/37/38.		
19. KEY WORDS (Continue on reverse side if necessary and identify by block number) Blast Shock Blast Simulation		
20. ABSTRACT (Continue on reverse side if necessary and identify by block number) This report summarizes the experimental data on air blast generation by detonable gas in balloons from various projects conducted by the staff of the General American Research Division for the Defense Nuclear Agency. Blast data, including peak overpressures, shock wave arrival times, positive phase durations and positive phase overpressure impulses, were gathered from these sources and are condensed and presented, together with descriptions of the balloons and the field operations.		

DD FORM 1473
1 JAN 73

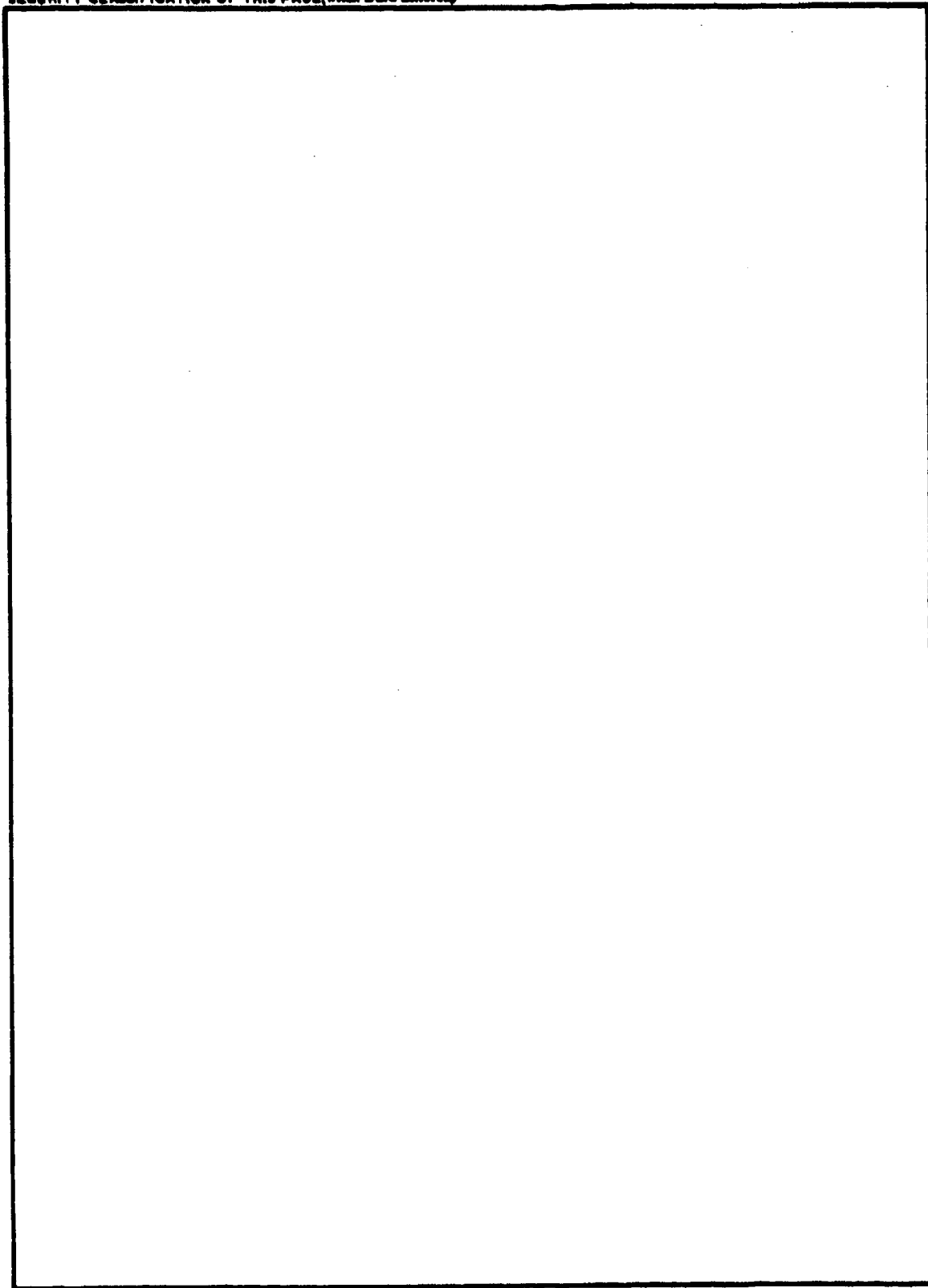
EDITION OF 1 NOV 65 IS OBSOLETE

UNCLASSIFIED

SECURITY CLASSIFICATION OF THIS PAGE (When Data Entered)

UNCLASSIFIED

SECURITY CLASSIFICATION OF THIS PAGE(When Data Entered)



UNCLASSIFIED

SECURITY CLASSIFICATION OF THIS PAGE(When Data Entered)

PREFACE

This report was prepared by the General American Research Division of the General American Transportation Corporation as Task 6 under Contract DNA 001-72-C-0058. This effort was supported by the Defense Nuclear Agency under NWED Subtask Code NA007 Work Unit Codes 28/37/38 and NWED Subtask Code V99QAXNA007. Col. M. Monaghan and Maj. R. Waters were the technical monitors. This work was done by the Applied Mechanics Group under the supervision of Dr. W. J. Byrne and the authors were ably assisted by Ms. M. T. Knobe and Mr. R. S. Koike.

TABLE OF CONTENTS

<u>Chapter</u>		<u>Page</u>
1	INTRODUCTION	7
2	EXPERIMENTAL CONSIDERATIONS	12
3	BLAST MEASUREMENTS	15
	3.1 Spherical Methane-Oxygen Balloons at Sea Level	15
	3.2 Hemispherical Propane-Oxygen Balloons	17
	3.3 Spherical Balloons at High Altitudes	18
	3.4 Shaped Balloons	19
4	DISCUSSION	21
	References	23

LIST OF ILLUSTRATIONS

<u>Figure</u>		<u>Page</u>
1	Schematic Illustration of Balloon Concept Used on Operation DISTANT PLAIN - Events 2, 2A, and 2B	24
2	Ballonet Balloon	25
3	Schematic Layout of Gas Handling System Used on Operation DISTANT PLAIN	26
4	10-Foot Diameter Sphere Filled with Oxygen and Methane Just Prior to Detonation at GARD's Ballistic Test Station (B.T.S.)	27
5	Fully Inflated 32-Foot Diameter Sphere at Suffield Experimental Station (S.E.S.)	28
6	Detonation of 32-Foot Diameter Sphere Containing Oxygen and Methane at 25-Foot Height-of-Burst (S.E.S.)	29
7	Cloud Rise Following Detonation of 32-Foot Diameter Sphere (S.E.S.)	30
8	32-Foot Diameter Sphere Filled with Helium and Air and Tethered at 25-Foot Height-of-Burst	31
9	110-Foot Diameter Sphere During Oxygen Fill Shortly before Failure (Event 2, Operation DISTANT PLAIN)	32
10	Fully Inflated 125-Foot Diameter Hemisphere Viewed from Technical Observation Point (Event 2A, Operation DISTANT PLAIN)	33
11	125-Foot Diameter Hemisphere During Oxygen Fill Showing Internal Ballonet (Event 2A, Operation DISTANT PLAIN)	34
12	125-Foot Diameter Hemisphere Viewed from Gas Loading Area During Propane Fill (Event 2A, Operation DISTANT PLAIN)	35
13	Detonation of 125-Foot Diameter Hemisphere Filled with Oxygen and Propane (EVENT 2A, OPERATION DISTANT PLAIN)	36
14	BRL High Altitude Simulating Blast Sphere	37
15	Fully Inflated Oxygen Chamber, Ballonet Balloon (BRL)	38
16	Fully Inflated Ballonet Balloon Containing Oxygen and Methane (BRL)	39

LIST OF ILLUSTRATIONS

(Continued)

<u>Figure</u>		<u>Page</u>
17	Nondimensional Peak Overpressure Versus Nondimensional Ground Range for an Oxygen-Methane Mixture Ratio of 1.5: Data for Spherical Balloons at a Height of Burst of $1.55 R_0$	40
18	Nondimensional Shock Arrival Time Versus Nondimensional Ground Range for an Oxygen-Methane Mixture Ratio of 1.5: Data for Spherical Balloons at a Height of Burst of $1.55 R_0$	41
19	Nondimensional Positive Phase Duration Versus Nondimensional Ground Range for an Oxygen-Methane Mixture Ratio of 1.5: Data for Spherical Balloons at a Height of Burst of $1.55 R_0$	42
20	Nondimensional Positive Phase Impulse Versus Nondimensional Ground Range for an Oxygen-Methane Mixture Ratio of 1.5: Data for Spherical Balloons at a Height of Burst of $1.55 R_0$	43
21	Nondimensional Peak Overpressure Versus Nondimensional Range for an Oxygen-Propane Mixture Ratio of 3.5: Data for Hemispherical Balloons	44
22	Nondimensional Shock Arrival Time Versus Nondimensional Range for an Oxygen-Propane Mixture Ratio of 3.5: Data for Hemispherical Balloons	45
23	Nondimensional Positive Phase Duration Versus Nondimensional Range for an Oxygen-Propane Mixture Ratio of 3.5: Data for Hemispherical Balloons	46
24	Nondimensional Positive Phase Impulse Versus Nondimensional Range for an Oxygen-Propane Mixture Ratio of 3.5: Data for Hemispherical Balloons	47
25	Nondimensional Peak Overpressure Versus Nondimensional Range for an Oxygen-Methane Mixture Ratio of 1.5: Blast Sphere Data for Spherical Balloons at Various Simulated Altitudes	48
26	Nondimensional Shock Arrival Time Versus Nondimensional Range for an Oxygen-Methane Mixture Ratio of 1.5: Blast Sphere Data for Spherical Balloons at Various Simulated Altitudes	49

LIST OF ILLUSTRATIONS
(Continued)

<u>Figure</u>		<u>Page</u>
27	Nondimensional Peak Overpressure Versus Nondimensional Range for an Oxygen-Hydrogen Mixture Ratio of 0.5: Blast Sphere Data for Spherical Balloons at Various Simulated Altitudes	50
28	Nondimensional Shock Arrival Time Versus Nondimensional Range for an Oxygen-Hydrogen Mixture Ratio of 0.5 Blast Sphere Data for Spherical Balloons at Various Simulated Altitudes	51
29	Nondimensional Peak Overpressure Versus Nondimensional Range for an Oxygen-Fuel Mixture Ratio of 1.0 (Fuel: 50% Hydrogen, 50% Methane): Blast Sphere Data for Spherical Balloons at Various Simulated Altitudes	52
30	Nondimensional Shock Arrival Time Versus Nondimensional Range for an Oxygen-Fuel Mixture Ratio of 1.0 (Fuel: 50% Hydrogen, 50% Methane): Blast Sphere Data for Spherical Balloons at Various Simulated Altitudes	53
31	Nondimensional Peak Overpressure Versus Nondimensional Range for an Oxygen-Methane Mixture Ratio of 1.5: AFWL DATA for 32-Foot Diameter Spherical Balloons at Kirtland Air Force Base	54
32	Nondimensional Shock Arrival Time Versus Nondimensional Range for an Oxygen-Methane Mixture Ratio of 1.5: AFWL Data for 32-Foot Diameter Spherical Balloons at Kirtland Air Force Base	55

LIST OF TABLES

<u>Table</u>		<u>Page</u>
1	Previous GARD Programs - Gas Detonations	8
2	Detonation Parameters for $P_0 = 1 \text{ ATM}$, $T_0 = 293.16^\circ\text{K}$ (68°F)	16

Chapter 1

INTRODUCTION

Detonable gas mixtures contained in balloons are capable of producing air blast environments which simulate high yield surface and high altitude bursts. The air blast produced by the gaseous detonation has a well-defined shock front and reproducible and predictable blast parameters.

General American Research Division (GARD) has conducted or participated in nine programs involving the use of detonable gas for blast simulation. Table 1 presents a list of these projects, source descriptions, yields, gas mixtures used, heights-of-burst and sponsoring agencies. The balloon configurations tested to date include spheres, spheres with an internal ballonet structure to speed up gas loading and to provide stability to the structure during loading, spheres with a ballonet to provide separation of the gases prior to launch for high altitude applications, hemispheres, hemispheres with an internal ballonet, shaped cylinders for long-duration pressure signatures and cylindrical half-disks for blast directing experimentation.

The research, development and testing of gas detonation phenomena for the creation of air blast environments has been conducted over the last ten years. Early work on the use of gaseous detonations as the driver in shock tubes led to an analytical treatment of the thermochemical processes associated with detonations (Johnson and Balcerzak, 1964). Detonation and blast characteristics were verified experimentally and some detonability limits as functions of mixture composition and initial pressure were established.

Balloons containing detonable gases were first tested in 1965 (Balcerzak, Johnson and Kurz, 1966). These initial tests with spherical balloons containing methane and oxygen verified the existence of spherical detonations, checked

Table 1
PREVIOUS GARD PROGRAMS - GAS DETONATIONS

<u>PROJECT</u>	<u>DEVICE</u>	<u>HEIGHT OF BURST</u>	<u>FUEL GAS</u>	<u>TNT EQUIVALENT</u>	<u>SPONSOR</u>
GAS EXPLOSION SIMULATION TECHNIQUE (AFWL)	32-FT DIAMETER SPHERICAL BALLOONS	130 TO 150 FT	METHANE	1000 LBS	DNA
HIGH ALTITUDE BLAST GENERATION SYSTEM II	10-FT DIAMETER SPHERICAL AND BALLOONET BALLOONS	35,000 FT SIMULATED	METHANE	8 LBS	BRL
SONIC BOOM SIMULATOR	SHAPED CYLINDRICAL ENVELOPES, UP TO 5-FT DIAMETER, UP TO 100-FT LENGTH	UP TO 20 FT	METHANE	UP TO 25 LBS	NASA
MIRACLE PLAY TEST SERIES	110-FT DIAMETER UNDERGROUND CAVITY	-2700 FT	METHANE	315 TONS	DNA
1500 PSI DYNAMIC LOAD SIMULATOR	40-FT LONG, 4-FT DIAMETER DETONATION TUBE	----	HYDROGEN, METHANE, HYDROGEN & METHANE	50 LBS	WES
BLAST DIRECTING TECHNIQUE	HALF-DISKS, UP TO 50-FT DIAMETER	SURFACE	METHANE	100 LBS	DASA
HIGH ALTITUDE BLAST GENERATION SYSTEM I	5 AND 10-FT DIAMETER SPHERICAL BALLOONS	50,000 TO 90,000 FT SIMULATED	HYDROGEN, METHANE, HYDROGEN & METHANE	LESS THAN 5 LBS	DASA
OPERATION DISTANT PLAIN	17 AND 125-FT DIAMETER HEMISPHERICAL BALLOONS	SURFACE	PROPANE	100 LBS AND 20 TONS	DASA
	110-FT DIAMETER SPHERICAL BALLOON	85 FT	METHANE	20 TONS	
DETONABLE GAS EXPLOSION	3, 5, 10, 13.5 AND 32-FT DIAMETER SPHERICAL BALLOONS	LESS THAN ONE BALLOON DIAMETER	METHANE	UP TO 1000 LBS	DASA

the accuracy of the analytical predictions, further delineated detonability limits and established proper field procedures. Tests were conducted using 3, 5, 10 and 13.5-foot diameter balloons. By utilizing the buoyancy of the methane-oxygen mixture, these spherical balloons were detonated at a height-of-burst of approximately three-quarters of one balloon diameter. Equivalent yields of up to 100 pounds of TNT were obtained.

Tests with 17-foot diameter hemispheres filled with a propane-oxygen mixture were conducted to verify the blast characteristics, detonation parameters, yield equivalences and detonability limits (Balcerzak, Johnson and Lucole, 1967).

Following these small-scale tests, a 32-foot diameter sphere containing a methane-oxygen mixture (equivalent yield of 1000 pounds of TNT) was detonated at a 25-foot height-of-burst at the Suffield Experimental Station, Ralston, Alberta, thus extending the capability of this technique to larger yields. Blast measurements from this event confirmed that normal cube root scaling was adequate.

Two large yield gas detonations, having equivalent yields of 20 tons of TNT, were than planned, as a part of the DISTANT PLAIN test series. Because of the size of the balloons and the requirement that these balloons be rapidly inflated to a stable configuration, an internal ballonet was incorporated in the design. The balloon would be rapidly inflated with air on one side of the ballonet to stabilize the overall balloon shape; then the air would be displaced as the detonable gas mixture was loaded. The tests planned were a methane-oxygen detonation in a 110-foot diameter sphere tethered at a height-of-burst of 85 feet and a propane-oxygen detonation in a 125-foot diameter hemisphere. The latter test was accomplished successfully. Pre-ignition of the methane-oxygen balloon led to a material

investigation to reduce the accumulation of static electricity on the balloon during loading of the detonable gases (Balcerzak, Johnson and Lucole, 1967).

An economic and technical study of the use of hemispherical detonable gas balloons as large yield explosive sources was carried out (Lucole and Balcerzak, 1968). Tests up to the equivalent of 100 tons of TNT were well within the state-of-the-art at that time and extension of this capability to larger yields was intimated. One of the major technical considerations was that the balloon design should be able to withstand winds up to 30 mph during the loading process and therefore the balloon must incorporate an internal ballonet. The conductive balloon material to be used in the manufacture of the large balloons was determined. Detonable gas loading rates of approximately 20,000 standard cubic feet per hour were realized during the DISTANT PLAIN tests. Significantly higher loading rates were obtained during the underground detonable gas explosion tests at the Tatum Salt Dome Test Site, Hattiesburg, Mississippi (MIRACLE PLAY Test Series, Klima and Byrne, 1971). The two tests conducted under this series were to simulate 315 tons of TNT in a 110-foot diameter spherical cavity 2700 feet below the surface. Significant advances in the gas loading system made it possible to achieve a loading rate of 400,000 standard cubic feet of gas per hour.

The detonation of buoyant detonable gases in spherical balloons to simulate high altitude blasts was a logical continuation. Use of the explosive itself for buoyancy overcomes one of the inherent difficulties in the use of TNT or other solid or liquid explosives. A technical and economic feasibility study of a high altitude blast generating system included the extension of the calculation of detonation and blast parameters to very low ambient pressures and an experimental program to verify the predictions

(Klima, Balcerzak and Johnson, 1967). Small balloons, filled with methane-oxygen, hydrogen-oxygen and methane-hydrogen-oxygen mixtures were detonated at simulated altitudes up to 90,000 feet in the Ballistic Research Laboratories' High Altitude Simulating Blast Sphere. Various methods of mixing the gases were evaluated. Design of the balloons, the gas loading and handling systems, launch and handling equipment, instrumentation and flight control, instrumentation recovery, and preliminary test site evaluation were other topics covered during this feasibility study. A study of the gas mixing for a particular balloon, the "bar-bell" balloonet balloon, designed to effect gas mixing during ascent to test altitude, confirmed that this design was effective (Fields, 1973).

Two other programs were performed to investigate the blast effects produced by the detonation of gases contained in shaped balloons. Both half-disks (Lucole and Balcerzak, 1968) and shaped cylinders (Strugielski, Fugelso, Holmes and Byrne, 1971) were tested.

Chapter 2

EXPERIMENTAL CONSIDERATIONS

The basic design of the balloon is rather straightforward. The exterior configuration of the balloon, normally constructed of mylar, can be made to the desired shape. Figure 1 shows two balloon configurations used for the spherical and hemispherical balloons during the DISTANT PLAIN test series. Because of the sizes of the balloons (110-foot diameter for the sphere and 125-foot diameter for the hemisphere), the balloon is rapidly inflated to its final shape with air on one side of an internal ballonet. After the air fill is complete, the detonable gas mixture is loaded on the other side of the ballonet and the air is forced out. Figure 2 shows a different ballonet designed to separate the gas components during the launch procedure for high altitude tests. The balloon is partially inflated at launch with methane in one compartment and oxygen in the other. When the balloon reaches the desired altitude (the balloon is naturally buoyant and will rise by itself), the balloon becomes fully inflated. During ascent the oxygen is released from its compartment, goes through the flexible duct entering the methane compartment at the top and mixes with the methane to create the detonable mixture.

Figure 3 shows schematically the gas handling system used to load the balloons on Operation DISTANT PLAIN. Methane and oxygen are passed from the storage tanks through a pipeline (partially above and partially below ground). Control of the gas loading rate is made through valves near the storage area.

A typical small (10-foot diameter) sphere detonated during the first experimental study is shown in Figure 4. The balloon material is a mylar-dacron scrim. Figure 5 shows the fully inflated 32-foot diameter sphere

filled with methane and oxygen and tested at the Suffield Experimental Station. The balloon material is a metallized mylar laminated on both sides of a dacron scrim. The equivalent yield of this balloon was 1000 pounds of TNT. The detonation of this balloon is shown in Figure 6. This particular detonation demonstrated that gas detonations of this type are symmetrical and produce clean, uniform shock fronts. It also confirmed the scaling from the smaller balloon detonations. The cloud rise (shown in Figure 7) indicates that the thermal plume from a gas detonation may be larger than from other explosions, which effect may be due to the high reaction temperatures and the size of the source.

Figure 8 shows the tethering test for the 110-foot diameter sphere. These tests, preliminary to the DISTANT PLAIN test series, were conducted to study the effects of lift, location of tethering points and addition of the ballonet structure on the deployment of the balloon. Figure 9 shows the 110-foot diameter sphere (Event 2, DISTANT PLAIN) during loading. The internal ballonet is seen in the middle, separating the air compartment (right side) and the detonable gas mixture (left side). The balloon was a mylar-dacron scrim with a calcium chloride coating to reduce static electricity build-up. The detonable gases were added in the following order: oxygen first (11 hours) followed by methane (gas mixing occurs by the turbulent methane plume rising through the oxygen). This balloon detonated prematurely after 4 hours of methane loading. A study into the cause of this led to the conclusion that static electricity had built up on the balloon surface during loading. A modified balloon material with silver grid wires to bleed off this electricity was later developed to reduce this hazard.

The 125-foot diameter hemispherical balloon, containing a detonable mixture of propane and oxygen and detonated as Event 2A of the DISTANT PLAIN

tests, is shown in Figure 10. The explosive energy released in this detonation simulated that of a surface burst of approximately 20 tons of TNT.

Figure 11 shows the balloon during the oxygen fill and illustrates the ballonnet structure. The air is on top of the ballonnet, oxygen below. Figure 12 shows the same balloon from the gas loading area. The detonation of this balloon is shown in Figure 13.

The Ballistic Research Laboratories' High Altitude Simulating Blast Sphere, used in the testing of balloon detonation properties at high altitudes, is shown in Figure 14. Detonability limits were obtained as a function of altitude and mixture composition for methane, hydrogen and methane-hydrogen as the fuel, and blast parameters were measured. Figure 15 shows the mylar-dacron scrim ballonnet balloon (Figure 2) with the oxygen chamber fully inflated, and Figure 16 shows the fully inflated balloon and flexible duct for the oxygen in front. This configuration operated successfully producing detonable mixtures and bona-fide detonations.

Chapter 3

BLAST MEASUREMENTS

Experimental and theoretical results for the various balloon detonations are summarized in this chapter. Peak overpressures and times-of-arrival are shown for each category of results and, where they were measured, positive phase durations and positive phase overpressure impulses. The scaling used on these graphs is that the distances are normalized by the balloon radius, R_0 , the pressures by the ambient pressure, P_0 , and the times by the quotient of the balloon radius with the ambient sound speed in air, a_0 . Correlation of this scaling with the standard cube root scaling with the explosive weight, W , is made by noting that $W = \kappa \rho E R_0^3$ where

$$\kappa = 2\pi/3 \text{ for a hemisphere}$$

$$\kappa = 4\pi/3 \text{ for a sphere}$$

$$\rho = \text{gas mixture density}$$

$$E = \text{energy released per unit mass}$$

Table 2 lists some theoretical detonation parameters for the four gas mixtures considered (at sea level, $P_0 = 1$ atmosphere, and $T_0 = 298.16^\circ\text{K}$ (68°F)). The entries in this table were generated from a computer program which evaluated the thermochemical equations describing a Chapman-Jouguet detonation (Klima and Fugelso, 1969).

3.1 Spherical Methane-Oxygen Balloons at Sea Level

Detonations of small spherical methane-oxygen balloons (balloon radii of 3, 5, 10 and 13.5 feet), tethered at a height-of-burst of approximately three quarters of one balloon diameter, were conducted at GARD's Ballistic Test Station (B.T.S.), (Balcerzak, Johnson and Kurz, 1966). A total of 13 balloons were detonated during this series. The mole ratio of oxygen to

Table 2

DETONATION PARAMETERS FOR $P_0 = 1 \text{ ATM}$, $T_0 = 293.16^\circ\text{K}$ (68°F)

DETONATION PRESSURE (ATM)	DETONATION TEMPERATURE ($^\circ\text{K}$)	FLOW VELOCITY (FT/SEC)	DETONATION VELOCITY (FT/SEC)	ENERGY RELEASE (10^6 FT-LB/LB)
$\text{O}_2/\text{CH}_4 = 1.5 \text{ BY VOLUME } (\rho_0 = .0664 \text{ LB/FT}^3)$				
31.5	3750	3700	8420	1.61
$\text{O}_2/\text{H}_2 = 0.5 \text{ BY VOLUME } (\rho_0 = .0311 \text{ LB/FT}^3)$				
19.1	3730	4150	9530	1.98
$\text{O}_2/\text{FUEL} = 1.0 \text{ BY VOLUME (FUEL: } 50\% \text{ CH}_4 + 50\% \text{ H}_2) (\rho_0 = .0532 \text{ LB/FT}^3)$				
26.8	3750	3810	8680	1.69
$\text{O}_2/\text{C}_3\text{H}_8 = 3.5 \text{ BY VOLUME } (\rho_0 = .0900 \text{ LB/FT}^3)$				
40.9	3770	3640	8270	1.55

methane was varied from 1.0 to 2.0. The maximum detonation occurred when the mole ratio was 1.5, in accordance with the thermochemical analysis. When this ratio is less than 1.3, no detonation occurs.

A 32-foot diameter sphere at a height-of-burst of 25 feet was successfully detonated at Suffield Experimental Station (S.E.S.), Ralston, Alberta. The oxygen-to-methane mole ratio was 1.5. The peak overpressures and the times-of-arrival of the shock wave are shown in Figures 17 and 18. Only those small balloons, for which the $O_2:CH_4$ mole ratio was 1.5, are shown. Figures 19 and 20 show the positive phase durations and positive phase overpressure impulses, measured only for the 32-foot diameter sphere. The theoretical curves are taken from AFWL numerical calculations (Whitaker, et. al., 1966).

3.2 Hemispherical Propane-Oxygen Balloons

Detonations of propane-oxygen mixtures in 17-foot diameter hemispheres were conducted at B.T.S. (Balcerzak, Johnson and Lucole, 1967). The mole ratios of oxygen to propane varied from 2 to 5. The optimum mole ratio for this gas mixture is 3.5. This gas mixture was detonated in a 125-foot diameter hemisphere as Event 2A in the DISTANT PLAIN test series.

The peak overpressures and the times-of-arrival of the shock wave are shown in Figures 21 and 22. Only those smaller balloons, for which the $O_2:CH_8$ mole ratio was 3.5, are included. The theoretical overpressures and times-of-arrival were calculated using GARD's computer code for spherically symmetric blast wave propagation. The positive phase durations and overpressure impulses, measured for Event 2A (Reisler, Ethridge, LeFevre and Giglio-Tos, 1971), are shown in Figures 23 and 24. No cratering near ground zero was observed and the directly transmitted ground shock was minimal.

3.3 Spherical Balloons at High Altitudes

A series of experimental determinations of the detonations of spherical balloons containing methane-oxygen, hydrogen-oxygen and methane-hydrogen-oxygen mixtures at reduced ambient pressure were made in the BRL High Altitude Simulating Blast Sphere. These shots simulated detonations at high altitudes from 35,000 to 90,000 feet (Klima, Balcerzak and Johnson, 1967, Fields, 1973). Detonability limits as a function of mixture composition and initial pressure were obtained. Optimum detonations were observed for an oxygen-to-methane mole ratio of 1.5, an oxygen-to-hydrogen mole ratio of 0.5 and an oxygen-to-fuel mole ratio of 1.0 where the fuel gas had equal parts of methane and hydrogen.

The peak overpressure versus range and time-of-arrival of the shock front versus range data for the methane-oxygen mixture are shown in Figures 25 and 26. Also shown on the first figure are the numerical predictions for sea level (Fields, 1973). As the simulated altitude increases (i.e., ambient pressure decreases), the expected normalized overpressure decreases slightly as the energy release shows a slight decrease with decreasing pressure. The experimental values of the overpressure-range data for the 35,000 and 50,000 foot altitude agree well with the predicted curves. The data for the higher altitudes are significantly below the predicted values. At simulated altitudes above 50,000 feet, the detonability limits have just been reached and to obtain a detonation, much larger detonators (72.4 grains PETN equivalent as compared to 7 grains) are required to initiate a detonation. The calculated time-of-arrival curve for sea level (Fields, 1973) is also shown on Figure 26. Similar measurements for the hydrogen-oxygen and methane-hydrogen-oxygen mixtures are shown on Figures 27 through 30. The theoretical predictions (Klima, Balcerzak and Johnson, 1967) are for 50,000 feet.

Several 32-foot diameter spherical balloons were detonated in a recent test series conducted at the Air Force Weapons Laboratory (Bunker, personal communication). The balloons were filled with a methane-oxygen mixture (oxygen-to-methane mole ratio of 1.5) and tethered at heights-of-burst of from 130 to 150 feet. Figures 31 and 32 show the free field peak overpressure and time of arrival data for the shots. The data cover larger ranges than the previous shots. For ranges up to $R/R_0 = 4$, the pressure gages, mounted from the tethering cables for the balloon, measured free field overpressures directly. The other set of data ($7 < R/R_0 < 10$) was from ground level gages which measured reflected shock overpressures. These latter values were reduced to the free field using the regular reflection coefficient of 2.2 (Brode, 1964) appropriate to the peak overpressure levels and angles of incidence at the location of the gages.

3.4 Shaped Balloons

Gas filled balloons with shapes other than spherical or hemispherical have been detonated to examine the shape effect. As a part of a program on blast directing studies with half-disk explosive arrays (Lucole and Balcerzak, 1968), four thin half-disks filled with methane-oxygen were detonated and pressure readings were made. Viewing this experiment in the horizontal plane, there is a triangular shaped region wherein the blast wave is planar and decays as if in one-dimensional flow (Fugelso and Fields, 1972). Overpressure measurements were made along the axis of symmetry within this triangular region and agreed to within 30% with the theoretical peak overpressure curve calculated from the similarity solution (Lindberg, 1967).

Detonations of methane-oxygen mixtures in thin, long cylindrical envelopes were performed to develop a pressure profile with a long-duration and low peak overpressure (this experimental procedure was used to simulate the pressure profile that might be expected in sonic booms), (Strugielski, Fugelso, Holmes and Byrne, 1971). Peak overpressures were measured along the axis of the balloon extended. A least square fit to the data shows that, approximately

$$\frac{P_M}{P_0} - 1 = 2.40 \left(\frac{R}{D}\right)^{-1.17}, \quad 50 < \frac{R}{D} < 800$$

where D is the diameter of the balloon and R is the distance along the axis of the balloon from the end.

The decay shape of the air blast wave can be controlled to a limited extent by control of the shape of the balloon. The desired pressure profile was the N-wave, which is a pressure-time history with an initial rapid compressive shock followed by a linear decay to pressure below ambient and terminated by a compressive shock, returning the pressure to ambient. This pressure signature is characteristic of the far field shocks generated by aircraft traveling at supersonic speeds. A balloon whose shape was cylindrical in the middle section capped by two truncated cones on the ends yielded a very good N-wave at a range where the initial peak overpressure was two pounds per square foot, a level which is characteristic of sonic boom signatures.

Chapter 4

DISCUSSION

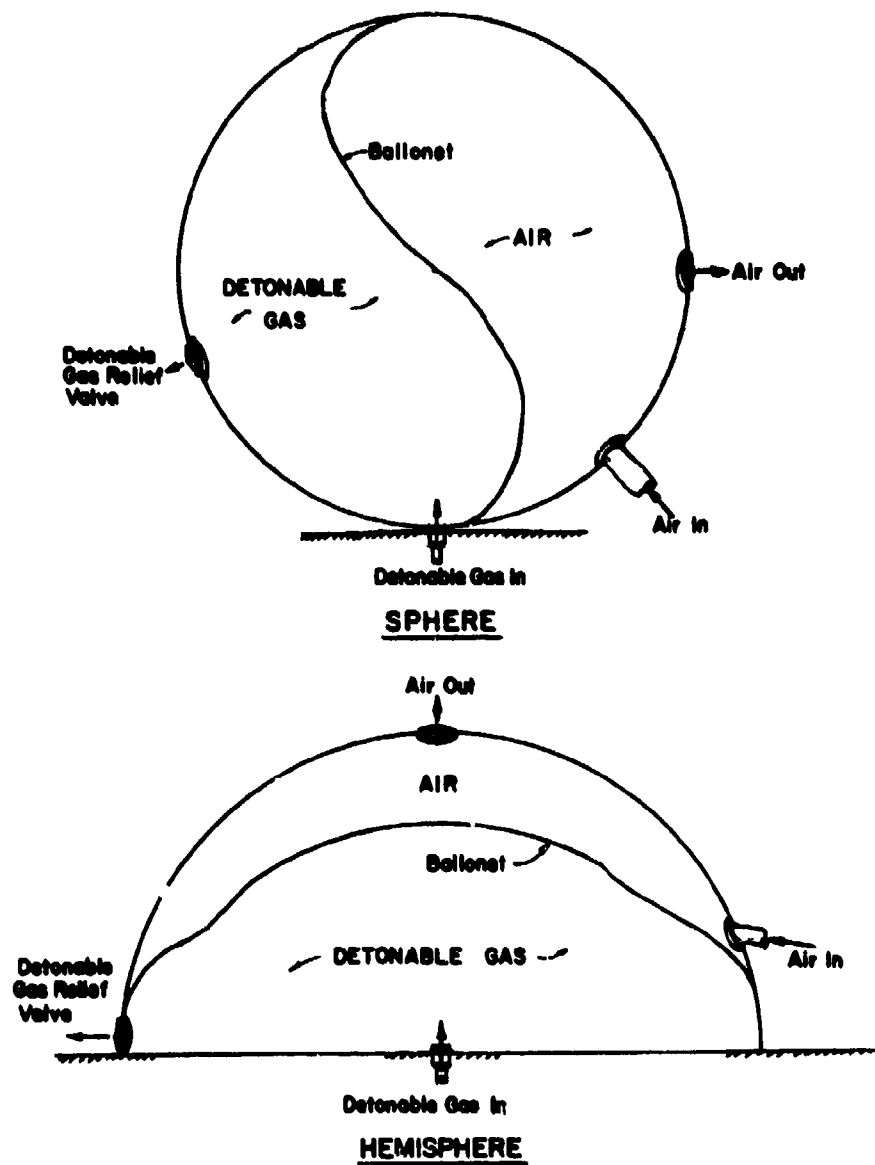
GARD, through a number of test programs, has established that detonable gases can simulate the blast environments of conventional and nuclear explosives. Potential advantages and disadvantages of this simulation technique are summarized below.

The technique generates a blast wave which has a well defined shock front and a subsequent blast pressure history which is remarkably free from turbulence and other minor irregularities. Comparable detonations of solid explosives such as TNT are characterized by turbulence caused by jetting and ejecta from irregular burning and detonation of the solid medium. The blast environment is very reproducible experimentally and can be analytically predicted with good accuracy through elementary blast and thermochemical codes developed for that purpose. The detonation pressures in the gas mixture are quite low; this limits the maximum overpressures that can be simulated. For propane-oxygen mixtures at atmospheric initial pressures, the maximum peak overpressure that can be effectively reached with a good pressure history is about 600 psi. The low detonation pressure minimizes the formation of craters and induces minimal directly transmitted ground motion. No toxic gases are generated during the detonation as only water, carbon monoxide and carbon dioxide are the reaction products. For large yield simulation, the low ambient pressure of the detonable mixture will require very large balloons and thus limit, in practice, the total yield that can be simulated. Both bouyant and non-bouyant gas mixtures are available; thus both surface bursts and high altitude or tethered (for controlled height-of-burst simulation) bursts can be readily attained. The experimental

configuration has important differences from solid H. E. explosive tests. No elaborate support structure for the explosives is needed. A remote gas loading system is required. This remote gas loading system implies that no direct explosive handling is necessary; however, this procedure requires a substantial amount of time to deploy the balloon.

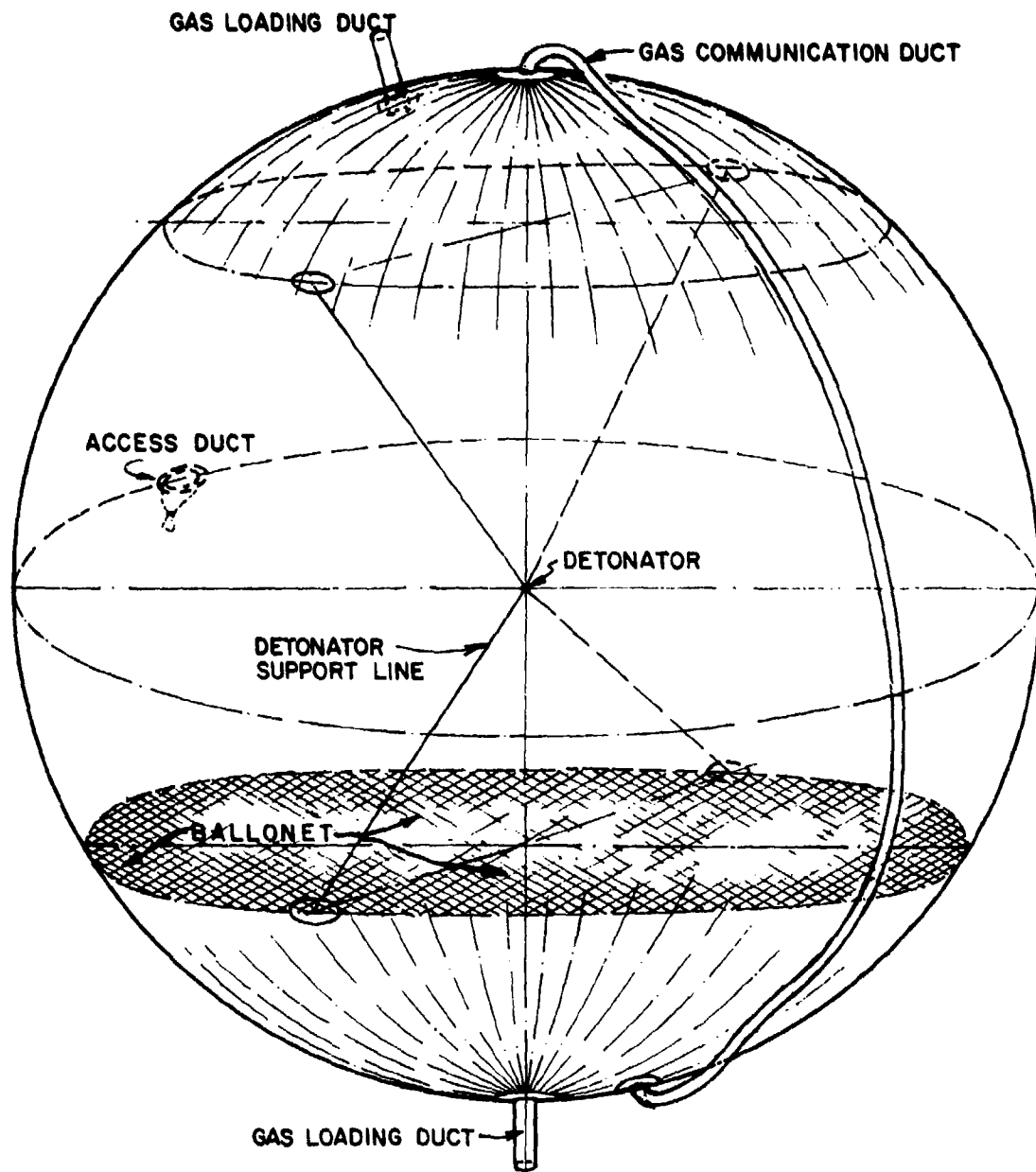
References

- Balcerzak, M.J., Johnson, M. R. and Kurz, F. R., "Nuclear Blast Simulation, Part I, Detonable Gas Explosion", DASA 1792-I, 1966.
- Balcerzak, M. J., Johnson, M. R. and Lucole, S. W., "Nuclear Blast Simulation, Detonable Gas Explosion, Operation DISTANT PLAIN", DASA 1945, 1967.
- Brode, H. L., "A Review of Nuclear Explosion Phenomenon Pertinent to Protective Construction", Rand Report R-PR-425, 1964.
- Fields, S. F., "High Altitude Blast Generation System: Detonable Gas Mixing Experiments", BRL CR 95, 1973.
- Fugelso, L. E. and Fields, S. F., "DIAL PACK Blast Directing Experiment", DNA 2756F, 1972.
- Johnson, M. R. and Balcerzak, M. J., "A Detonation Tube Driver for Producing Hypersonic Flows in a Shock Tube", Proc. Third Hypervelocity Techniques Symposium, 1964.
- Klima, R. J., Balcerzak, M. J. and Johnson, M. R., "High Altitude Blast Generation System, Part I, Theoretical and Experimental Analysis", DASA 2303-I, 1967.
- Klima, R. J. and Balcerzak, M. J., "High Altitude Blast Generation System, Part II, Design and Economic Study", DASA 2303-II, 1967.
- Klima, R. J. and Byrne, W. J., "Underground Detonable Gas Explosions, MIRACLE PLAY Test Series", DASA 2676, 1971.
- Klima, R. J. and Fugelso, L. E., "Theory and Operation Manual, 1500 psi Dynamic Load Simulator", Final Report, Contract DACA 39-68-C-0047, Waterways Experimental Station, 1969.
- Lindberg, H. E., "Simulation of Transient Surface Loads Using Plane, Cylindrical and Spherical Blast Waves", SRI, Poulter Laboratories Technical Report 002-67, 1967.
- Lucole, S. W. and Balcerzak, M. J., "Blast and Shock Simulation, Blast Directing Technique", DASA 2150, 1968.
- Lucole, S. W. and Balcerzak, M. J., "High Yield Detonable Gas Explosions, SLEDGE Technique", DASA 2302, 1968.
- Reisler, R. E., Ethridge, N. H., LeFevre, D. P. and Giglio-Tos, L., "Air Blast Measurements from the Detonation of an Explosive Gas Contained in a Hemispherical Balloon (Operation DISTANT PLAIN, Event 2A)", BRL MR 2108, 1971.
- Strugielski, R. T., Fugelso, L. E., Holmes, L. B. and Byrne, W. J., "The Development of a Sonic Boom Simulator with Detonable Gases", NASA CR-1844, 1971.
- Whitaker, W. A., Nawrocki, E. A., Needham, C. E. and Troutman, W. W., "A Preliminary Report of Theoretical Calculations of the Phenomenology of H. E. Detonations", Operation DISTANT PLAIN Preliminary Report, Vol. I, DASA 1876-I, 1966.



SCHEMATIC ILLUSTRATION OF BALLOON CONCEPT USED ON OPERATION DISTANT PLAIN - EVENTS 2, 2a, and 2b.

Figure 1



BALLONET BALLOON.

Figure 2



Figure 4 10-FOOT DIAMETER SPHERE FILLED WITH OXYGEN AND METHANE JUST PRIOR TO DETONATION AT GARD'S BALLISTIC TEST STATION (B.T.S.).

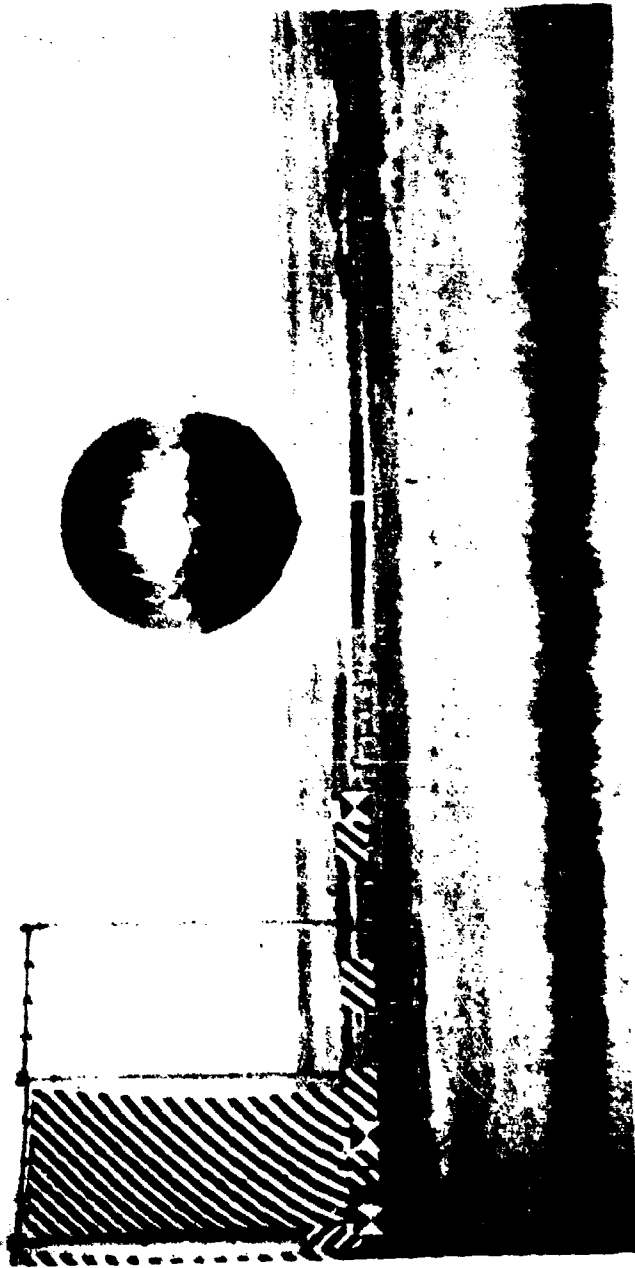


Figure 5 FULLY INFLATED 32-FOOT DIAMETER SPHERE AT SUFFIELD EXPERIMENTAL STATION (S.E.S.).



Figure 6 DETONATION OF 32-FOOT DIAMETER SPHERE CONTAINING OXYGEN AND METHANE
AT 25-FOOT HEIGHT-OF-BURST (S.E.S.).



Figure 7 CLOUD RISE FOLLOWING DETONATION OF 32-FOOT DIAMETER SPHERE (S.E.S.).



Figure 8 32-FOOT DIAMETER SPHERE FILLED WITH HELIUM AND AIR AND TETHERED AT 25-FOOT HEIGHT-OF-BURST.

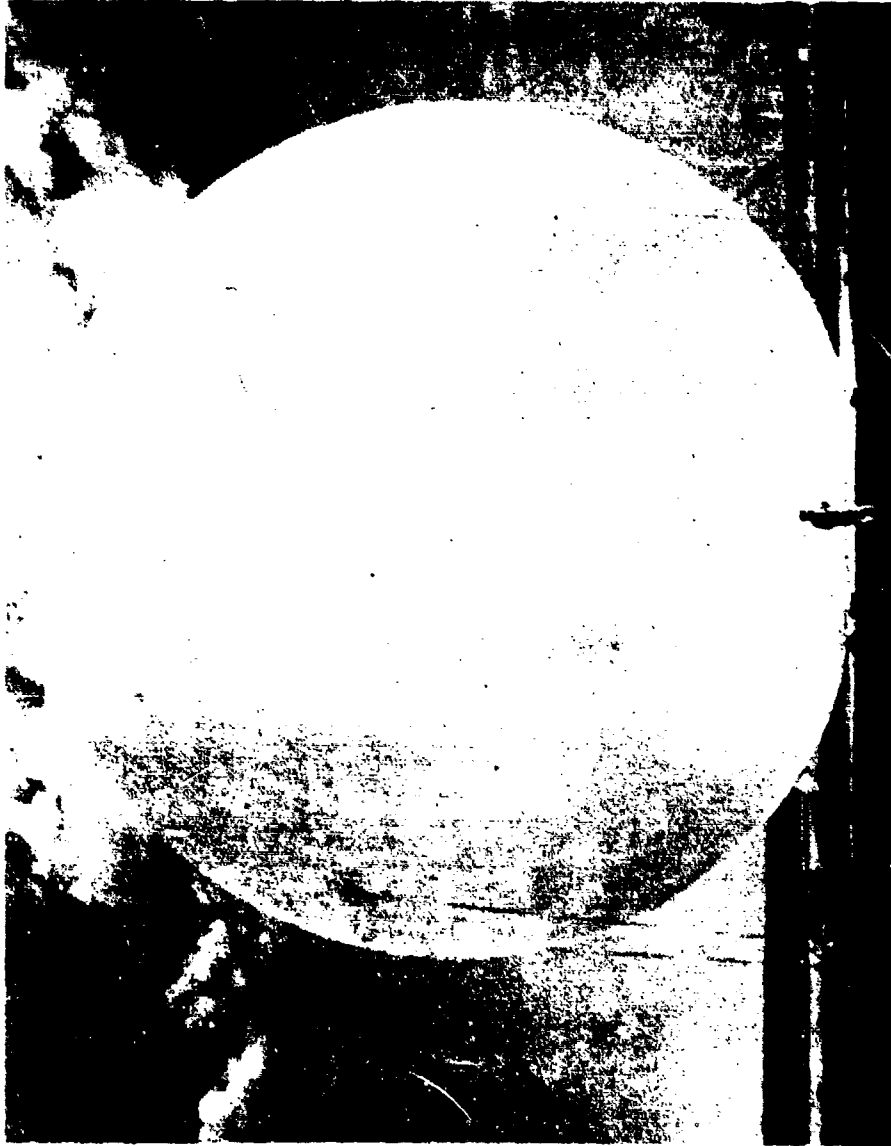


Figure 9 110-FOOT DIAMETER SPHERE DURING OXYGEN FILL SHORTLY BEFORE FAILURE
(EVENT 2, OPERATION DISTANT PLAIN).



Figure 10 FULLY INFLATED 125-FOOT DIAMETER HEMISPHERE VIEWED FROM TECHNICAL OBSERVATION POINT (EVENT 2a, OPERATION DISTANT PLAIN).

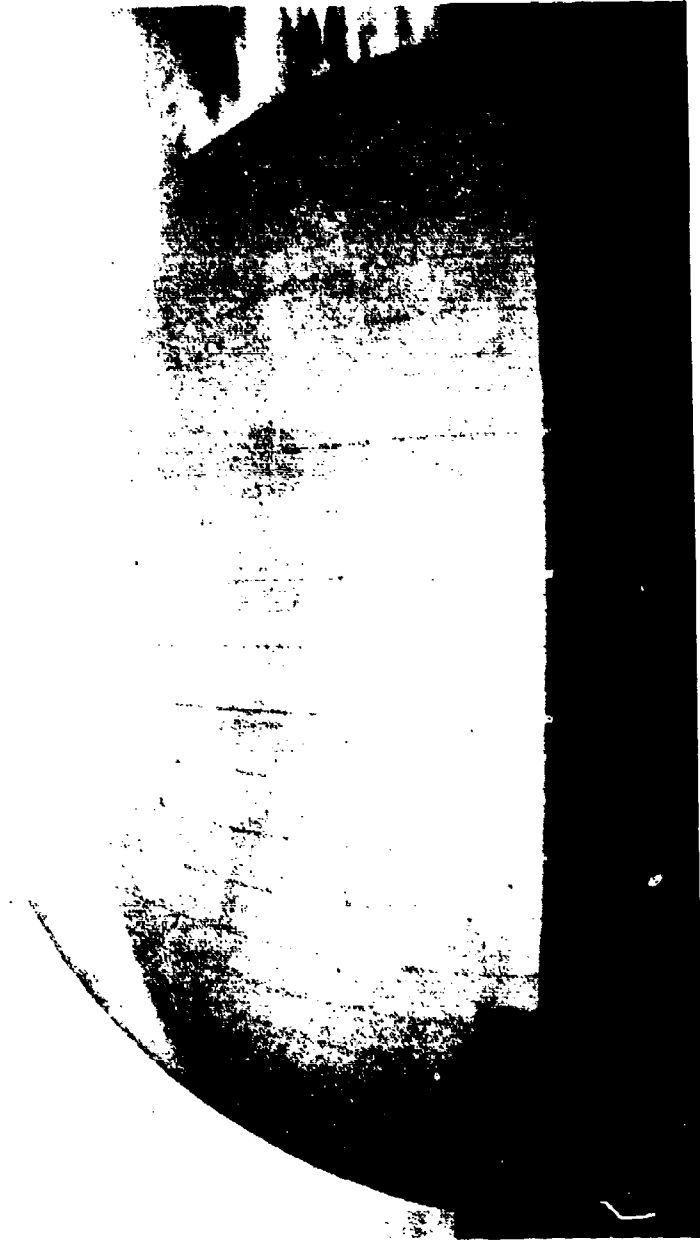


Figure 11 125-FOOT DIAMETER HEMISPHERE DURING OXYGEN FILL SHOWING INTERNAL BALLONNET
(EVENT 2a, OPERATION DISTANT PLAIN).



Figure 12 125-FOOT DIAMETER HEMISPHERE VIEWED FROM GAS LOADING AREA DURING PROPANE FILL (EVENT 2a, OPERATION DISTANT PLAIN).



Figure 13 DETONATION OF 125-FOOT DIAMETER HEMISPHERE FILLED WITH OXYGEN AND PROPANE (EVENT 2a, OPERATION DISTANT PLAIN).



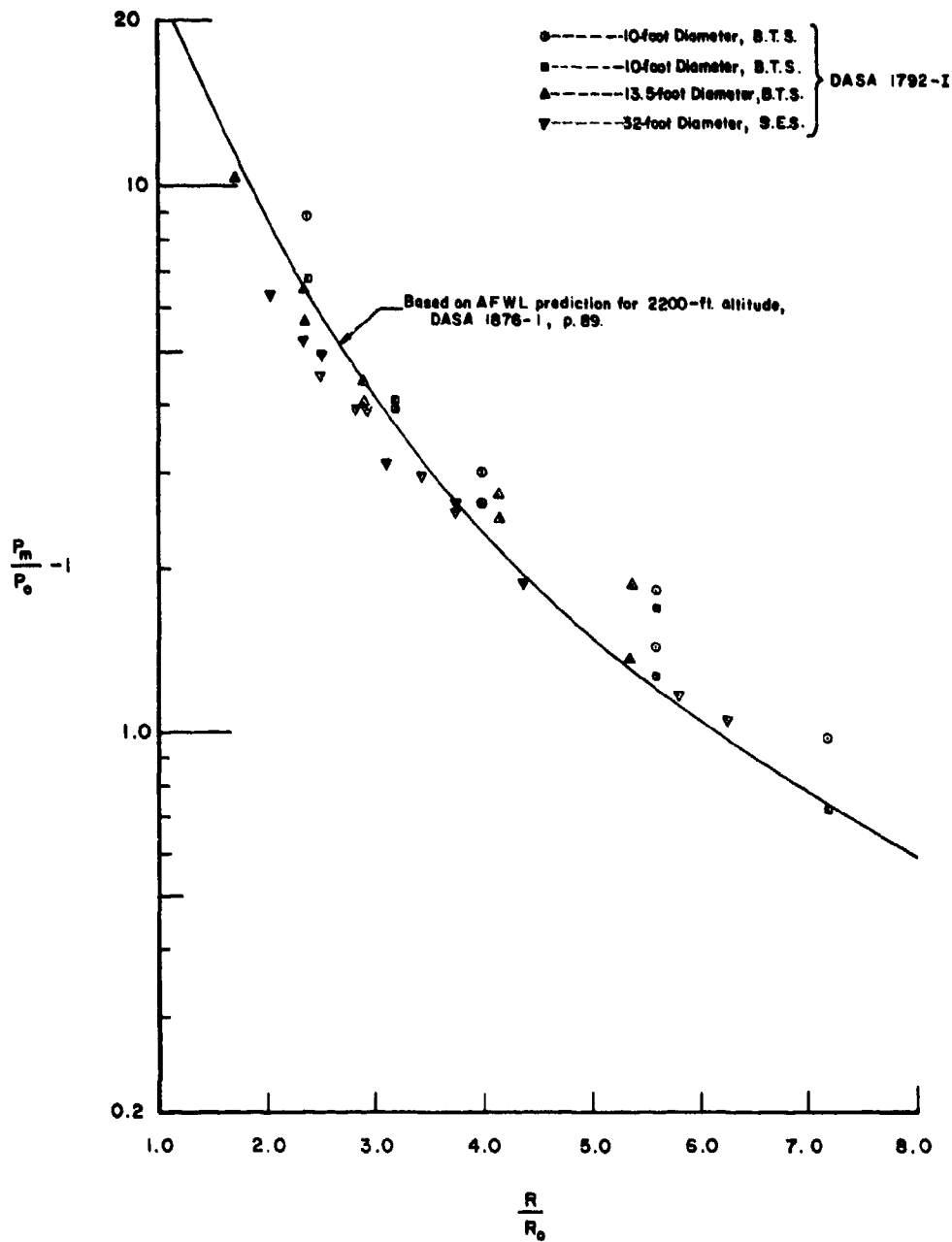
Figure 14 BRL HIGH ALTITUDE SIMULATING BLAST SPHERE.



Figure 15 FULLY INFLATED OXYGEN CHAMBER, BALLONET BALLOON (BRL).

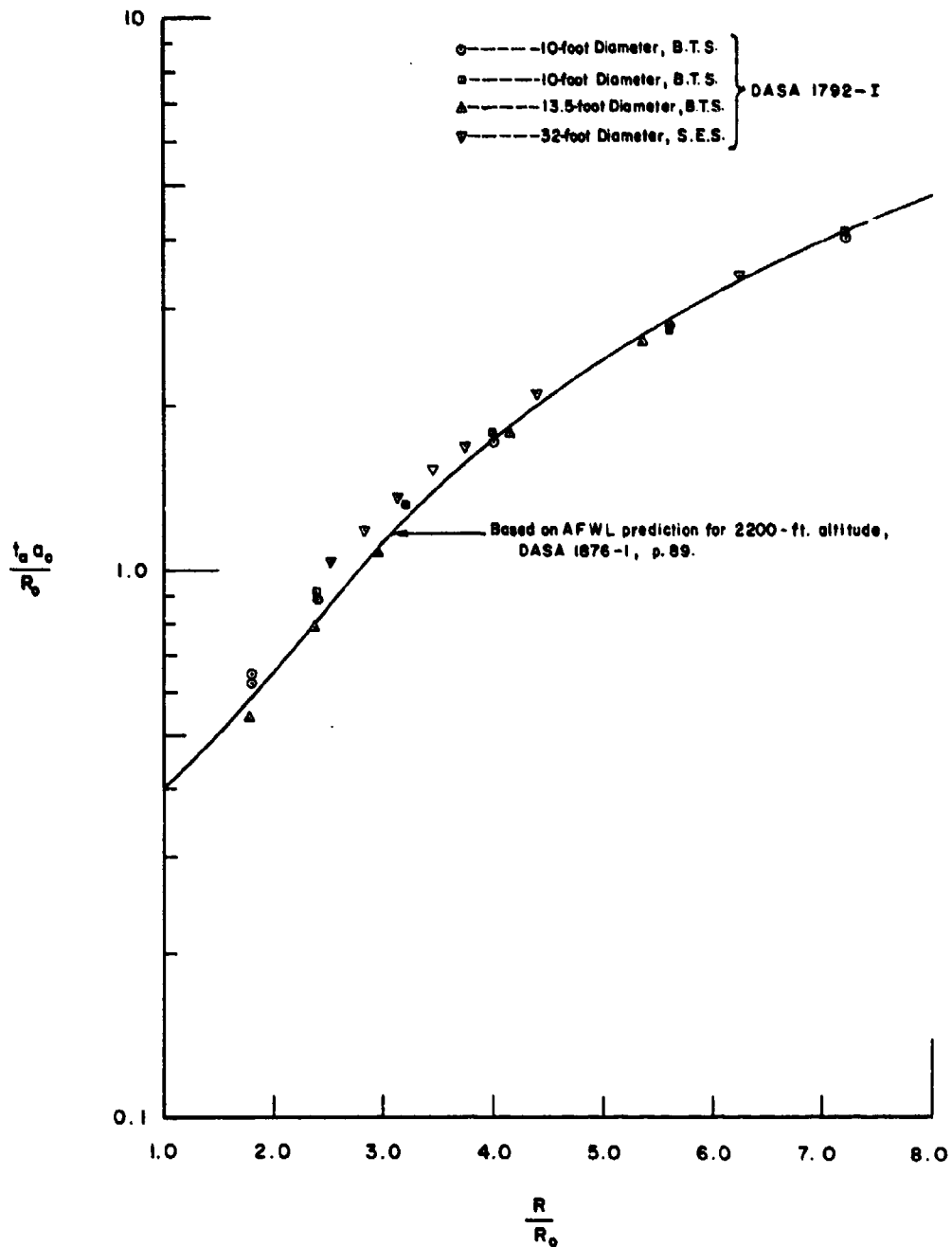


Figure 16 FULLY INFLATED BALLONET BALLOON CONTAINING OXYGEN AND METHANE (BRL).



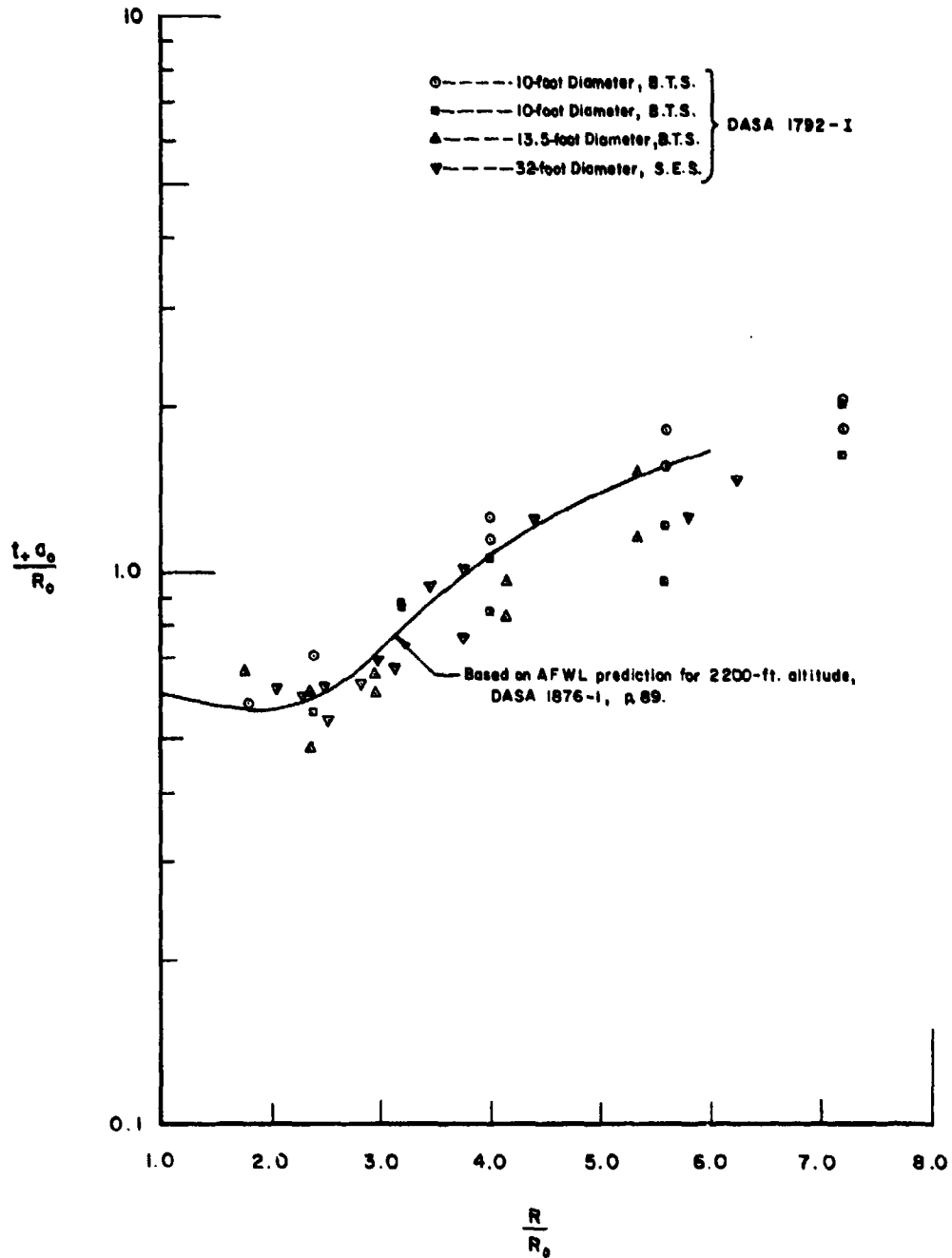
NONDIMENSIONAL PEAK OVERPRESSURE VERSUS NONDIMENSIONAL GROUND
 RANGE FOR AN OXYGEN - METHANE MIXTURE RATIO OF 1.5. DATA FOR SPHERICAL
 BALLOONS AT A HEIGHT OF BURST OF $1.55 R_0$.

Figure 17



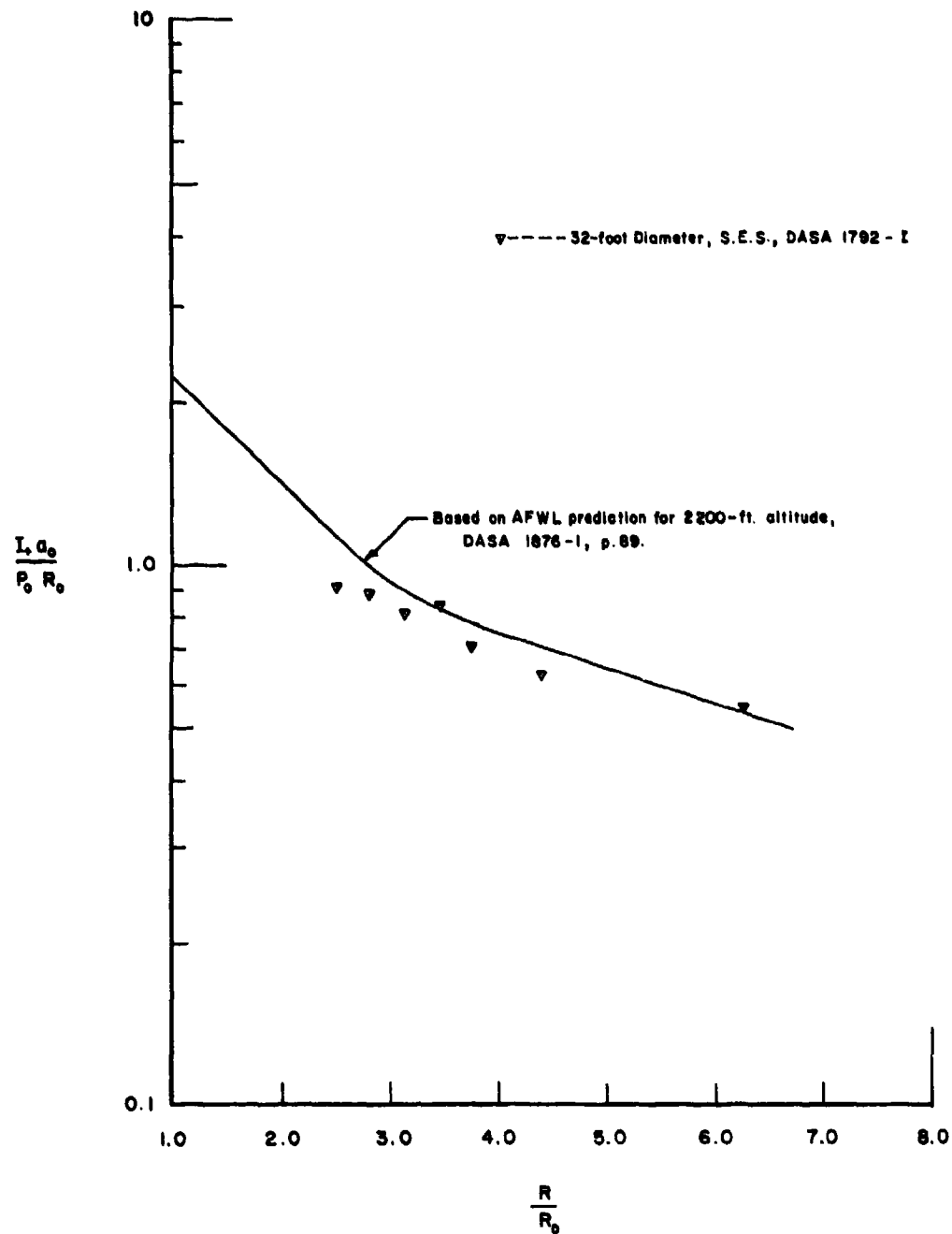
NONDIMENSIONAL SHOCK ARRIVAL TIME VERSUS NONDIMENSIONAL GROUND RANGE FOR AN OXYGEN-METHANE MIXTURE RATIO OF 1.5. DATA FOR SPHERICAL BALLOONS AT A HEIGHT OF BURST OF $1.55 R_0$.

Figure 18



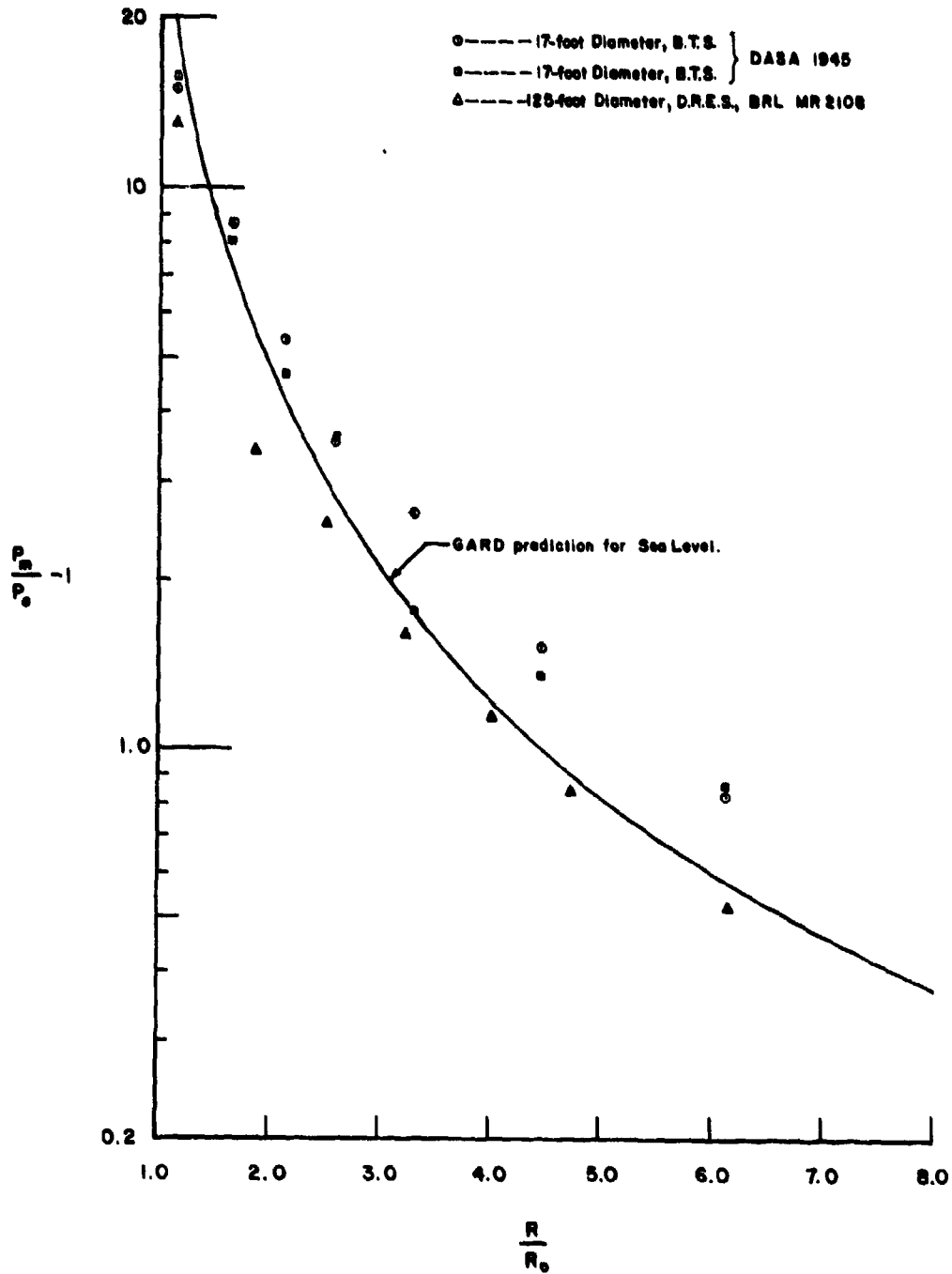
NONDIMENSIONAL POSITIVE PHASE DURATION VERSUS NONDIMENSIONAL GROUND
 RANGE FOR AN OXYGEN-METHANE MIXTURE RATIO OF 1.5: DATA FOR SPHERICAL
 BALLOONS AT A HEIGHT OF BURST OF $1.55 R_0$.

Figure 19



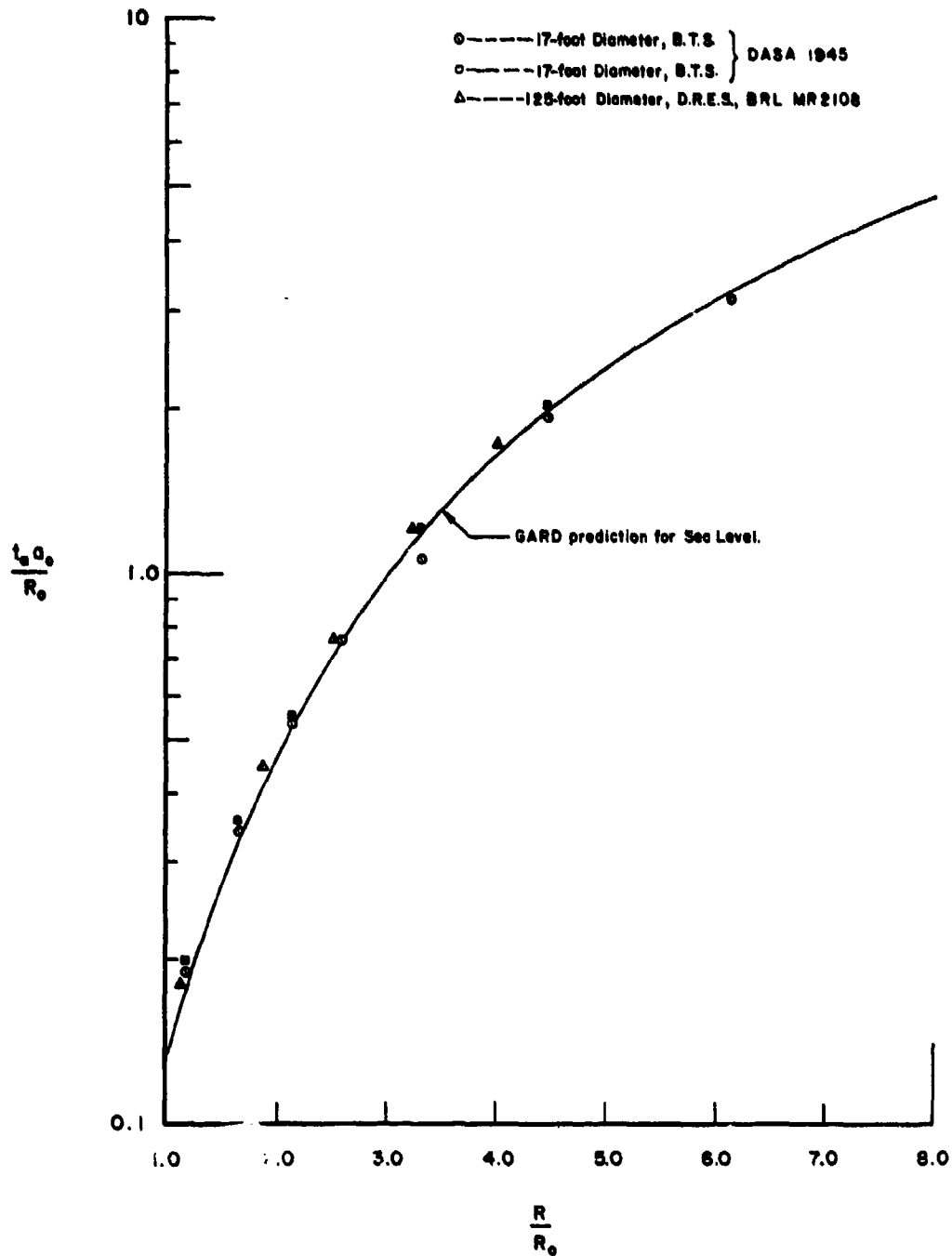
NONDIMENSIONAL POSITIVE PHASE IMPULSE VERSUS NONDIMENSIONAL GROUND RANGE FOR AN OXYGEN-METHANE MIXTURE RATIO OF 1.5; DATA FOR SPHERICAL BALLOONS AT A HEIGHT OF BURST OF $1.55 R_0$.

Figure 20



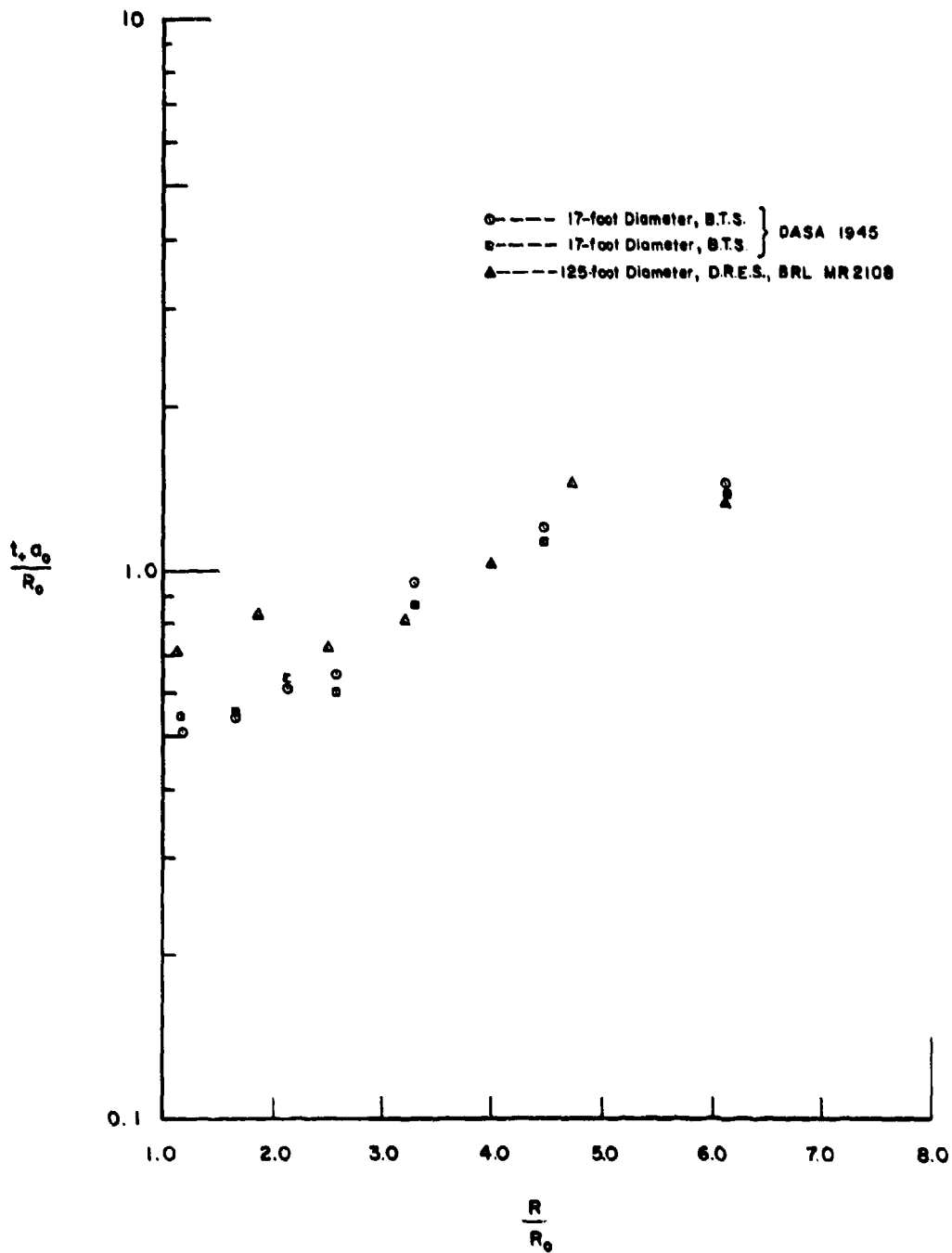
NONDIMENSIONAL PEAK OVERPRESSURE VERSUS NONDIMENSIONAL RANGE
 FOR AN OXYGEN-PROPANE MIXTURE RATIO OF 3.5; DATA FOR HEMISPHERICAL
 BALLOONS.

Figure 21



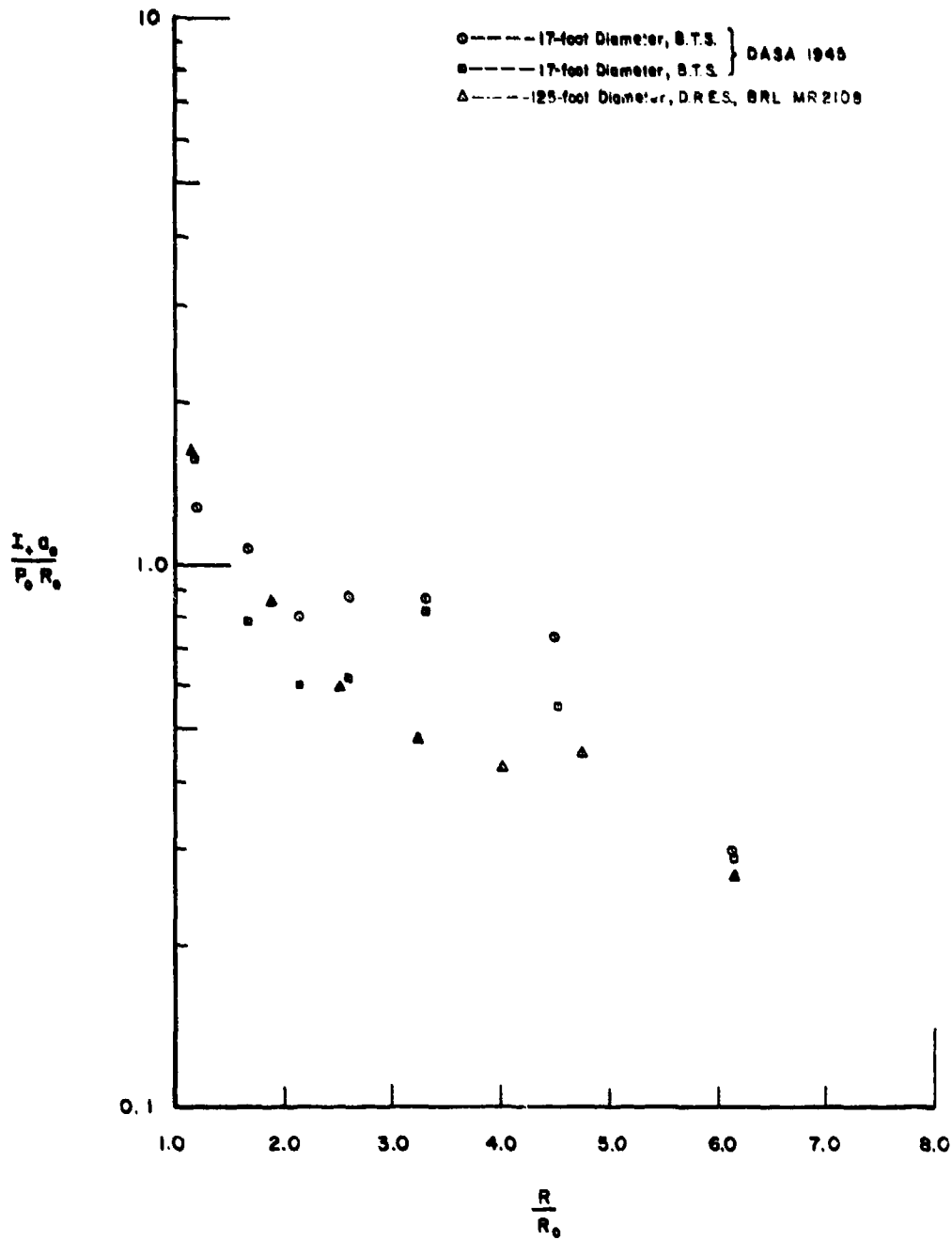
NONDIMENSIONAL SHOCK ARRIVAL TIME VERSUS NONDIMENSIONAL RANGE FOR AN OXYGEN-PROPANE MIXTURE RATIO OF 3.5: DATA FOR HEMISPHERICAL BALLOONS.

Figure 22



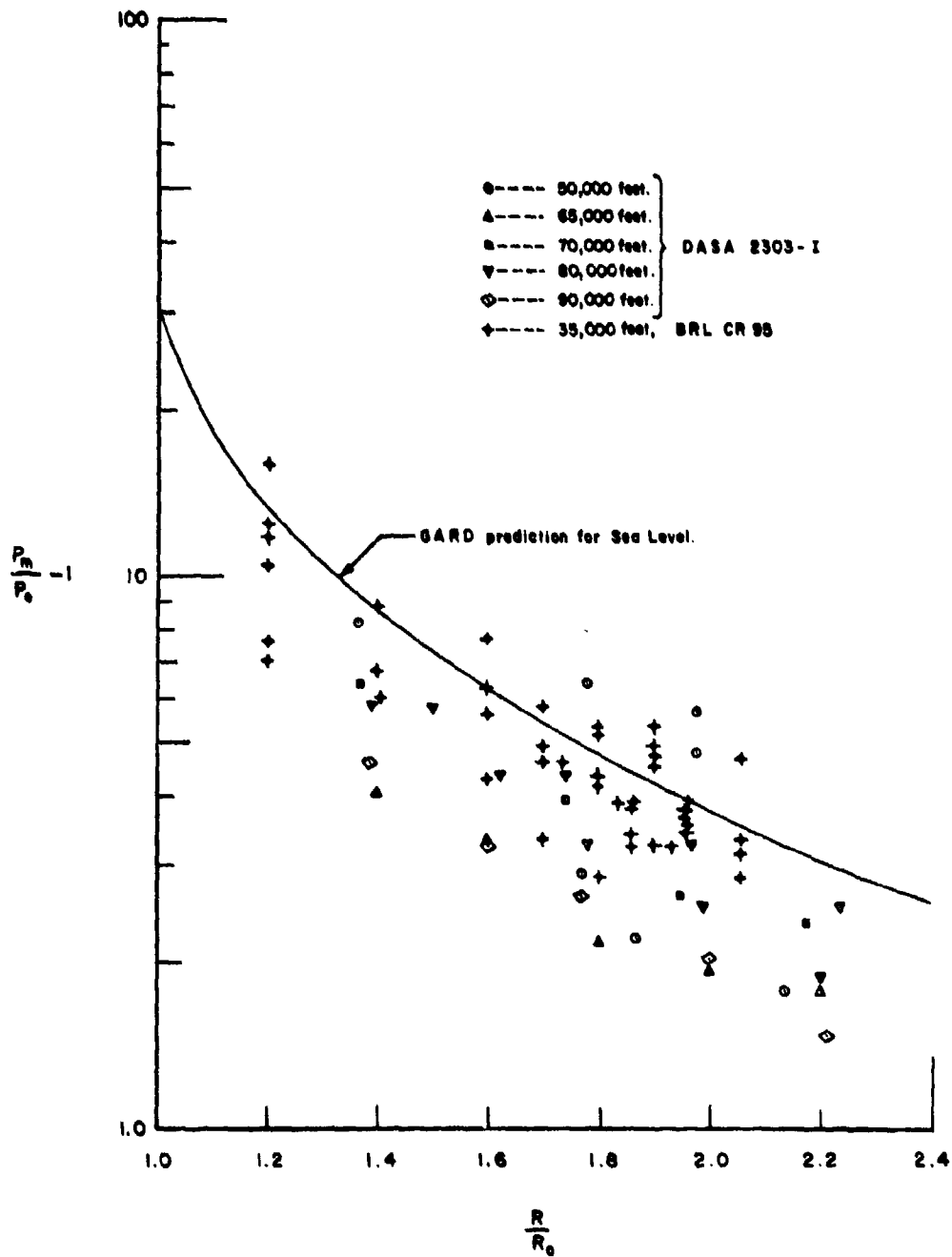
NONDIMENSIONAL POSITIVE PHASE DURATION VERSUS NONDIMENSIONAL RANGE
 FOR AN OXYGEN-PROPANE MIXTURE RATIO OF 3.5; DATA FOR HEMISPHERICAL
 BALLOONS.

Figure 23



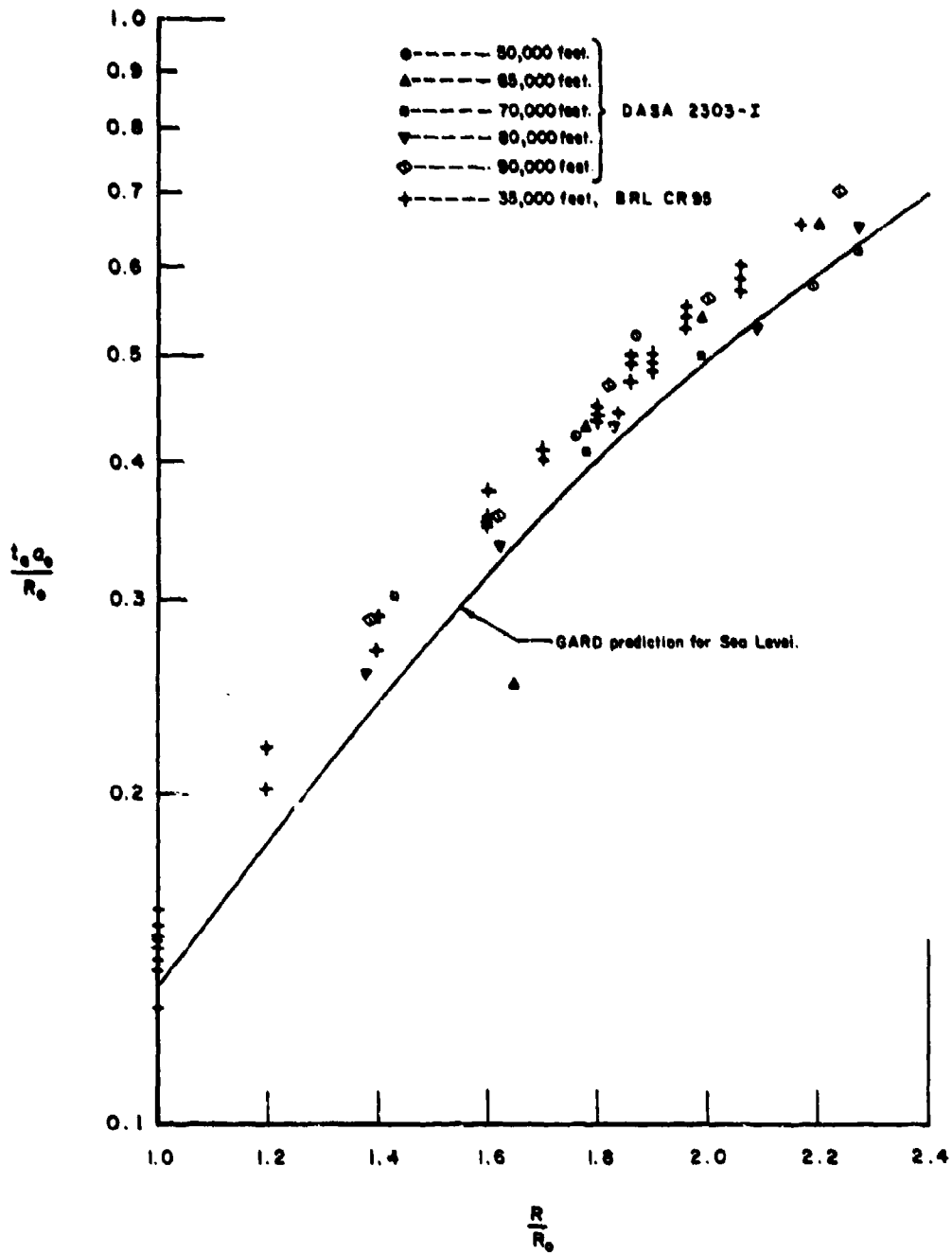
NONDIMENSIONAL POSITIVE PHASE IMPULSE VERSUS NONDIMENSIONAL RANGE FOR AN OXYGEN-PROPANE MIXTURE RATIO OF 3.5: DATA FOR HEMISPHERICAL BALLOONS.

Figure 24



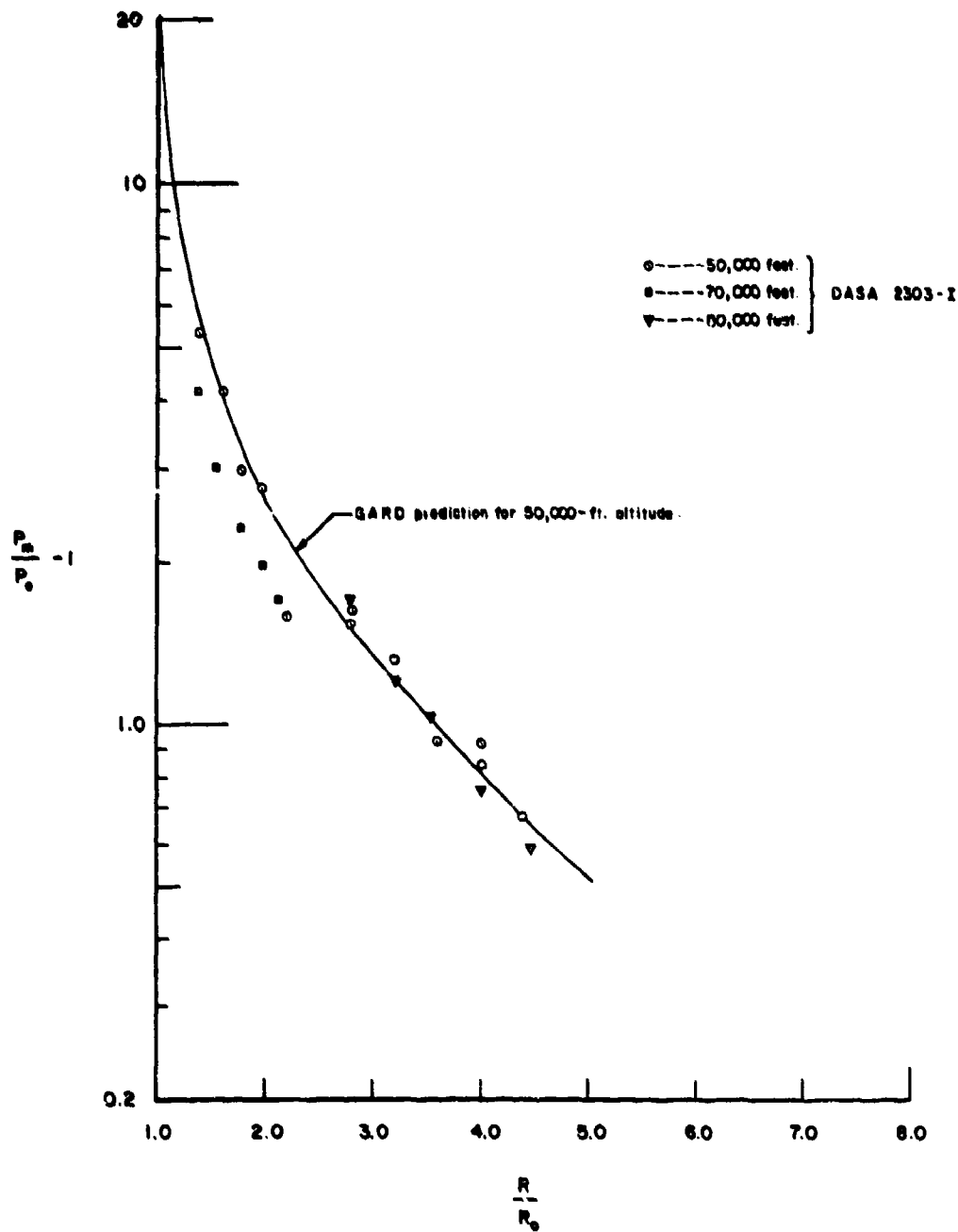
NONDIMENSIONAL PEAK OVERPRESSURE VERSUS NONDIMENSIONAL RANGE FOR
 AN OXYGEN - METHANE MIXTURE RATIO OF 1.5 : BLAST SPHERE DATA FOR
 SPHERICAL BALLOONS AT VARIOUS SIMULATED ALTITUDES.

Figure 25



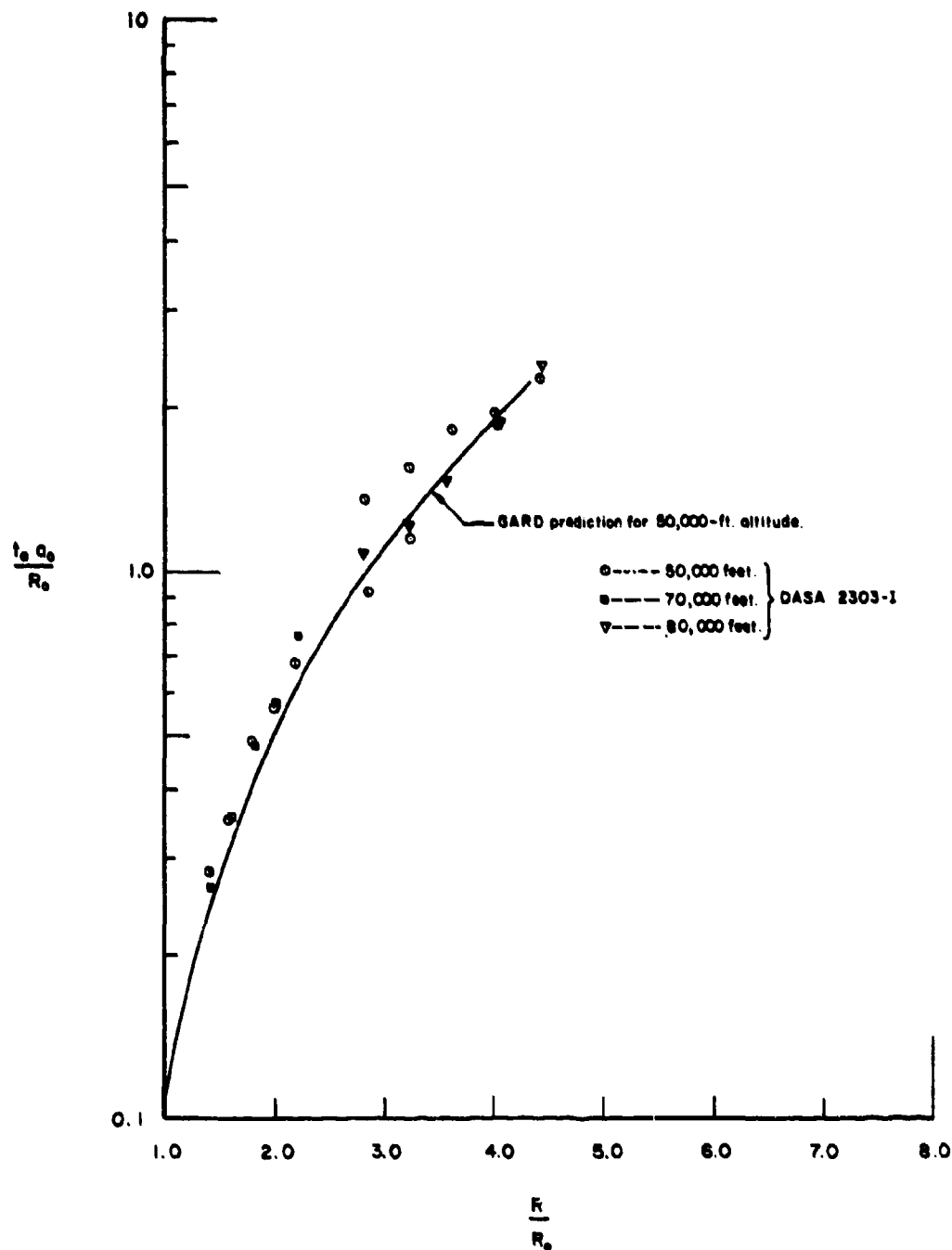
NONDIMENSIONAL SHOCK ARRIVAL TIME VERSUS NONDIMENSIONAL RANGE FOR AN OXYGEN-METHANE MIXTURE RATIO OF 1.5: BLAST SPHERE DATA FOR SPHERICAL BALLOONS AT VARIOUS SIMULATED ALTITUDES.

Figure 26



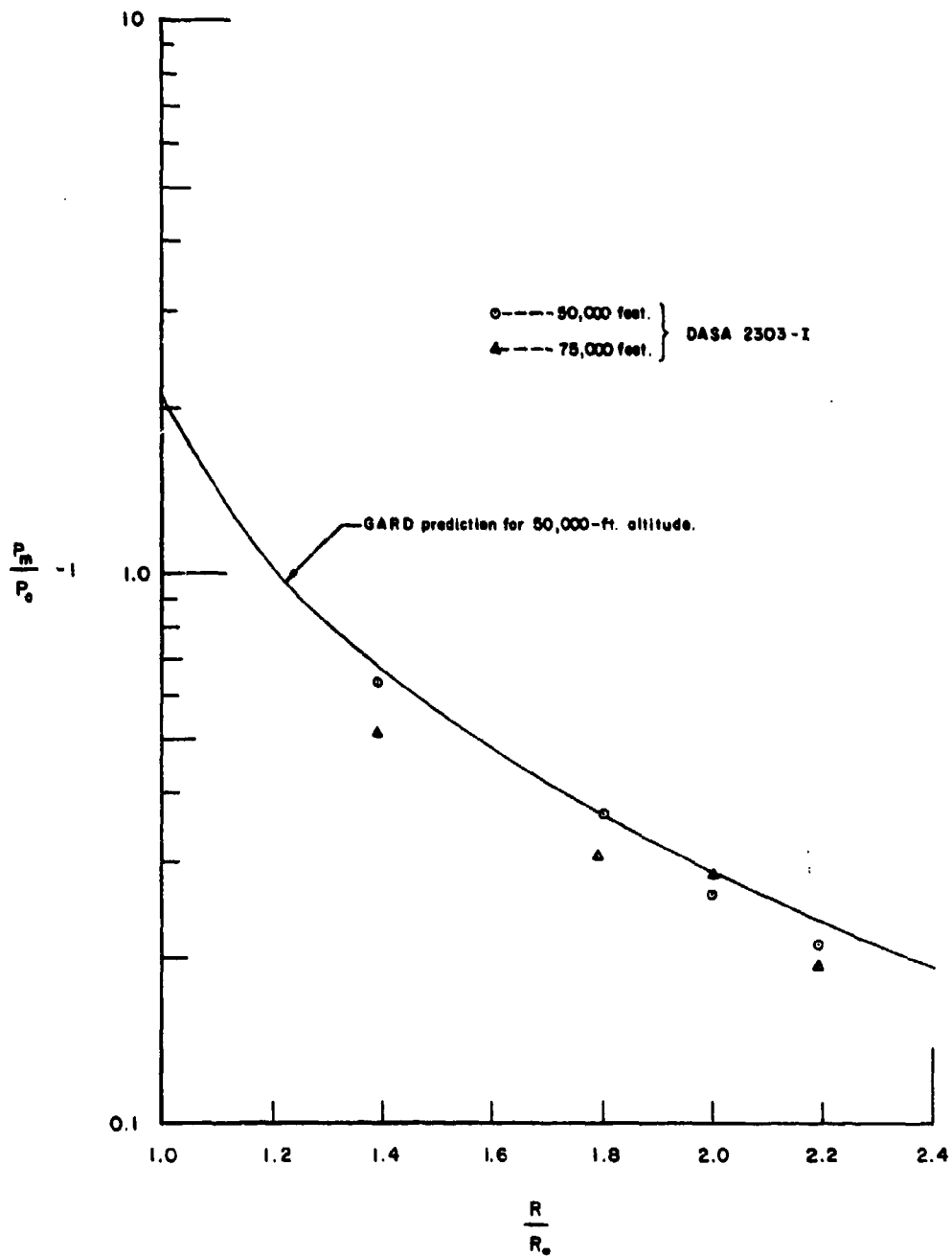
NONDIMENSIONAL PEAK OVERPRESSURE VERSUS NONDIMENSIONAL RANGE
 FOR AN OXYGEN-HYDROGEN MIXTURE RATIO OF 0.5: BLAST SPHERE DATA
 FOR SPHERICAL BALLOONS AT VARIOUS SIMULATED ALTITUDES.

Figure 27



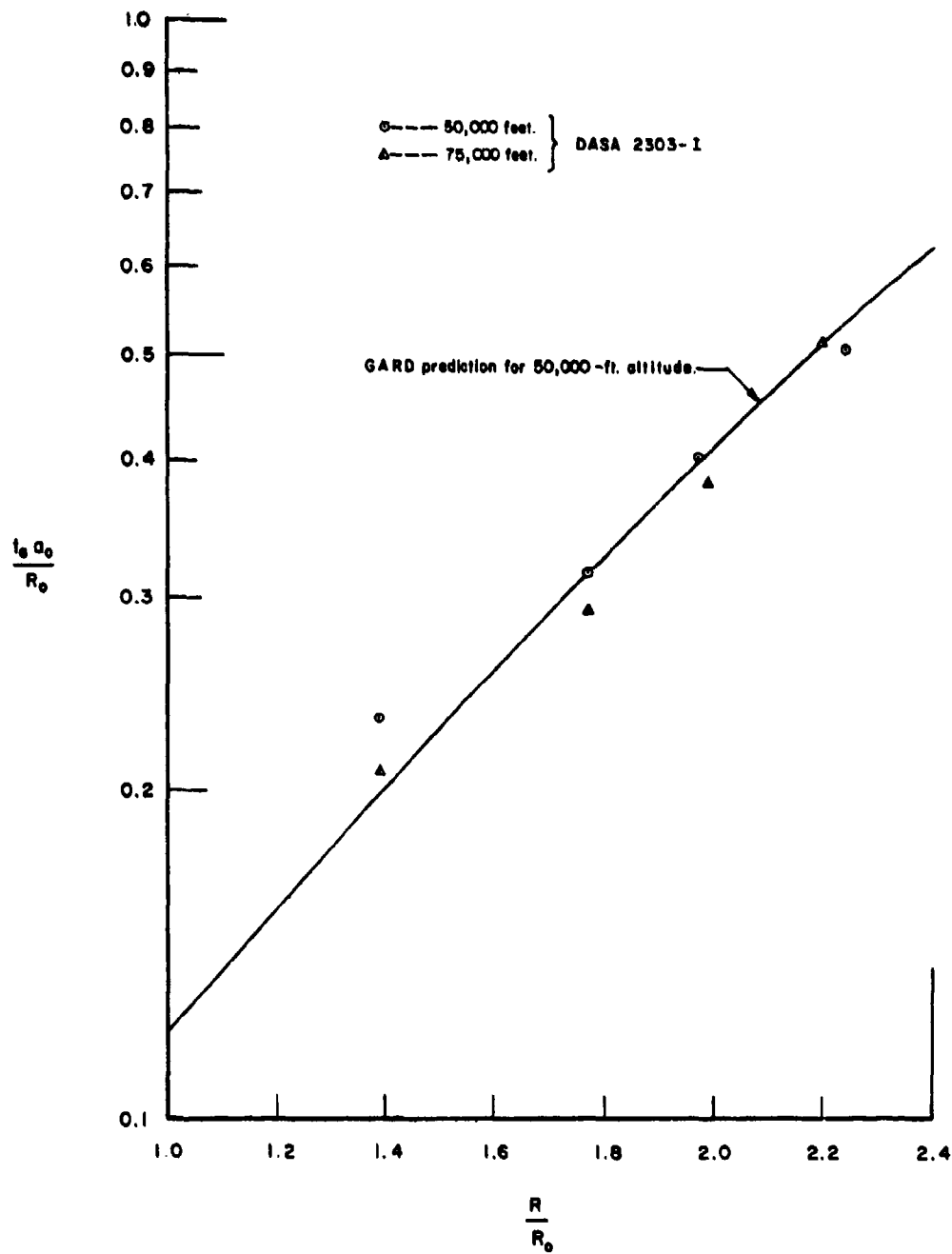
**NONDIMENSIONAL SHOCK ARRIVAL TIME VERSUS NONDIMENSIONAL RANGE
 FOR AN OXYGEN-HYDROGEN MIXTURE RATIO OF 0.5: BLAST SPHERE DATA
 FOR SPHERICAL BALLOONS AT VARIOUS SIMULATED ALTITUDES.**

Figure 28



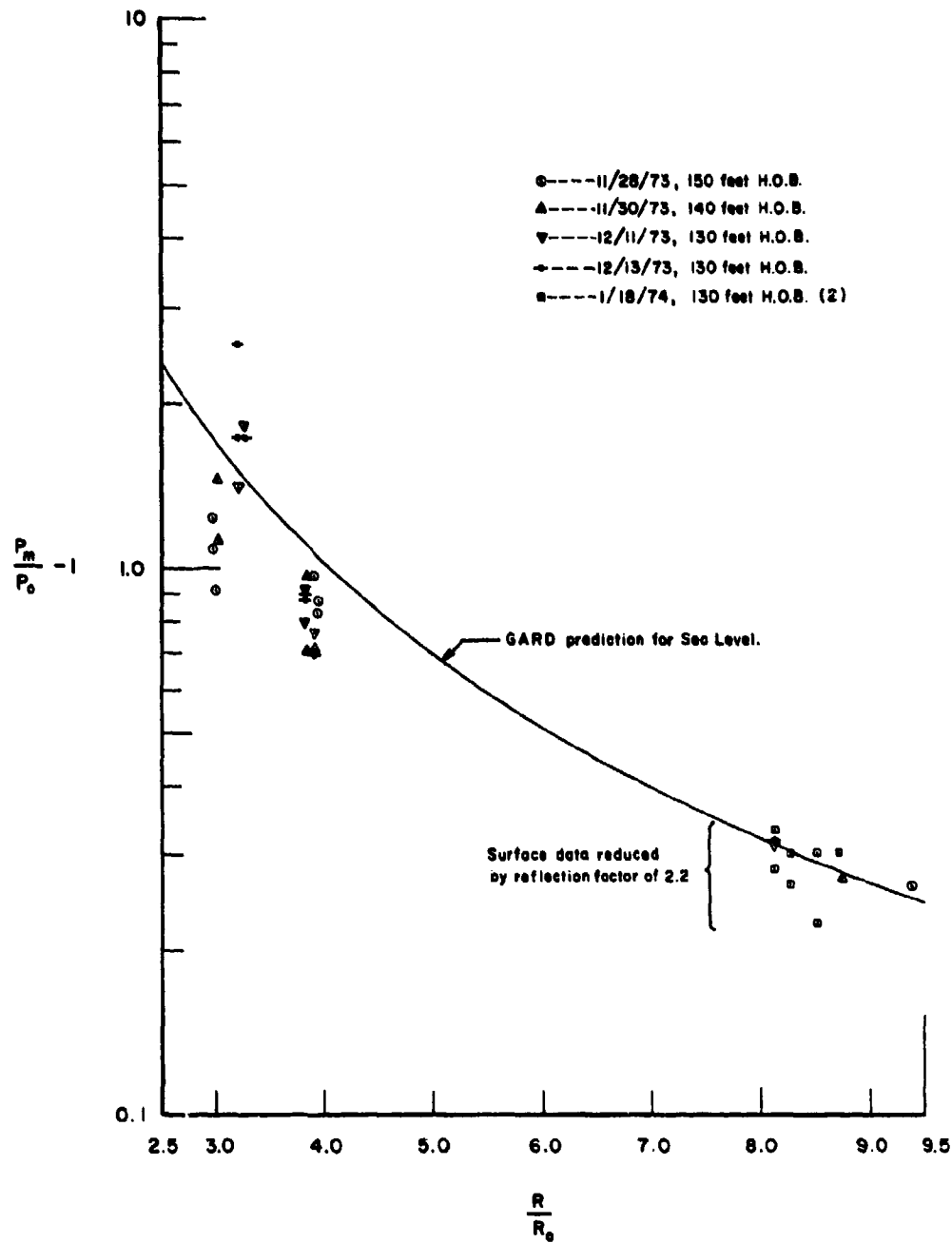
NONDIMENSIONAL PEAK OVERPRESSURE VERSUS NONDIMENSIONAL RANGE FOR
 AN OXYGEN-FUEL MIXTURE RATIO OF 1.0 (FUEL : 50% HYDROGEN, 50% METHANE):
 BLAST SPHERE DATA FOR SPHERICAL BALLOONS AT VARIOUS SIMULATED ALTITUDES.

Figure 29



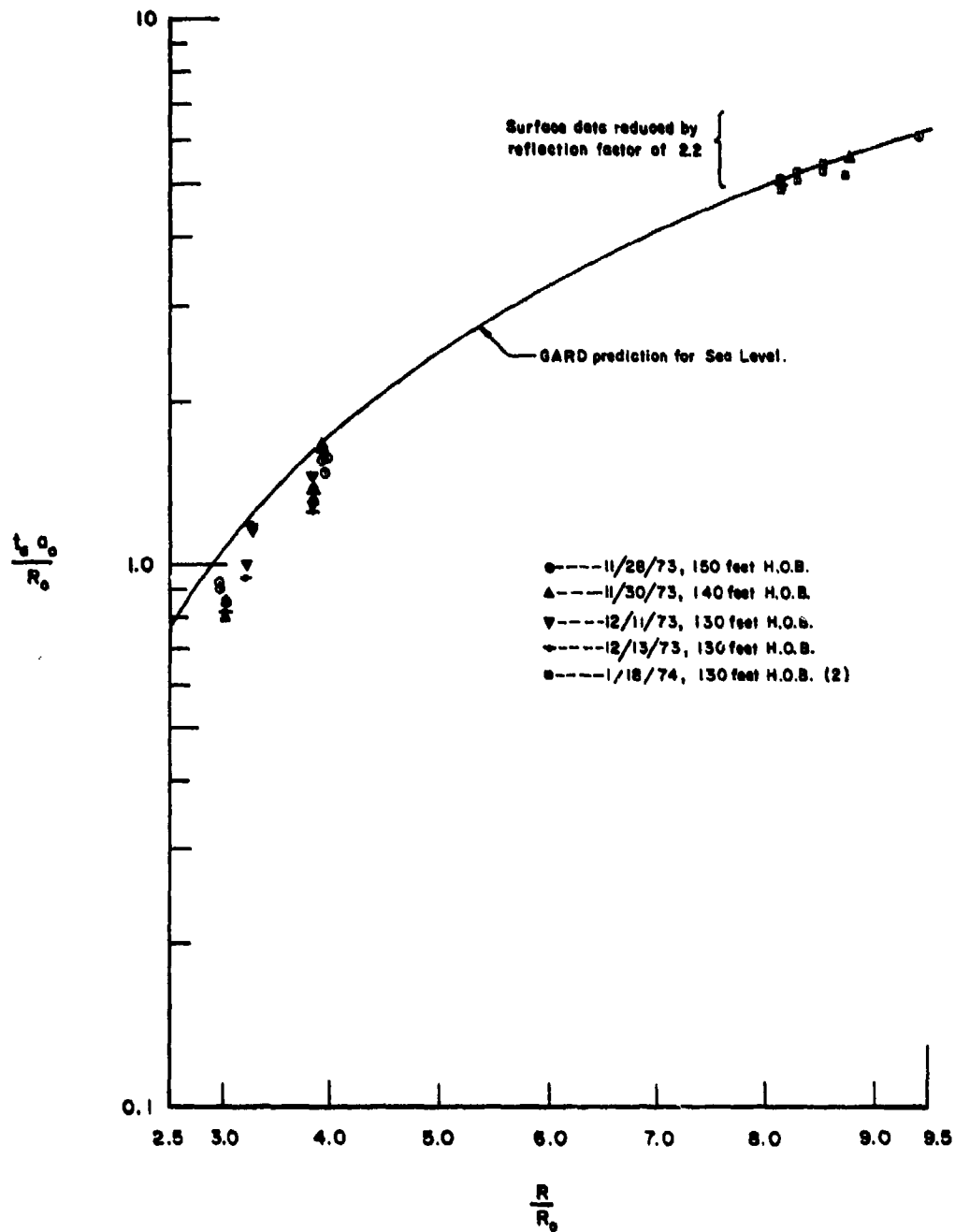
**NONDIMENSIONAL SHOCK ARRIVAL TIME VERSUS NONDIMENSIONAL RANGE FOR
 AN OXYGEN-FUEL MIXTURE RATIO OF 1.0 (FUEL: 50% HYDROGEN, 50% METHANE);
 BLAST SPHERE DATA FOR SPHERICAL BALLOONS AT VARIOUS SIMULATED ALTITUDES,**

Figure 30



NONDIMENSIONAL PEAK OVERPRESSURE VERSUS NONDIMENSIONAL RANGE FOR AN OXYGEN-METHANE MIXTURE RATIO OF 1.5 : AFWL DATA FOR 32-FOOT DIAMETER SPHERICAL BALLOONS AT KIRTLAND AIR FORCE BASE.

Figure 31



NONDIMENSIONAL SHOCK ARRIVAL TIME VERSUS NONDIMENSIONAL RANGE FOR AN OXYGEN-METHANE MIXTURE RATIO OF 1.5: AFWL DATA FOR 32-FOOT DIAMETER SPHERICAL BALLOONS AT KIRTLAND AIR FORCE BASE.

Figure 32

DISTRIBUTION LIST

DEPARTMENT OF DEFENSE

Defense Documentation Center
Cameron Station
2 cy ATTN: TC

Director
Defense Nuclear Agency
ATTN: DDST
ATTN: STSI (Archives)
2 cy ATTN: STTL, Technical Library
2 cy ATTN: SPSS

Director of Defense Research & Engineering
ATTN: Dep Dir (Info & Space Systems)
ATTN: Asst Dir Strat Weapons
ATTN: Dep Dir (Strategic Systems)

Commander
Field Command
Defense Nuclear Agency
ATTN: FCTA

Interservice Nuclear Weapons School
ATTN: Document Control

DEPARTMENT OF THE ARMY

Director
Ballistic Missile Defense Prog Office
ATTN: Dr. John Shea

Chief of Research & Development
Department of the Army
ATTN: Technical Library

Director
Explosive Excavation Research Laboratory
ATTN: Technical Library

Commander
Harry Diamond Laboratories
ATTN: AMXDO-NP

Commander
U. S. Army Engineer Center
ATTN: ATSEN-SY-L

Director
U. S. Army Engineer Waterways Experiment Station
ATTN: Leo Ingram
ATTN: Library Branch

Commander
U. S. Army Nuclear Agency
ATTN: CDINS-E

Director
U. S. Army Ballistic Research Laboratories
2 cy ATTN: Technical Library

DEPARTMENT OF THE NAVY

Officer-in-Charge
Civil Engineering Laboratory
Naval Construction Battalion Center
ATTN: Code L31
ATTN: Stan Takahaski

DEPARTMENT OF THE NAVY (Continued)

Commander
Naval Ship Research and Development Center
ATTN: Code L42, 3, Library

Commander
Naval Surface Weapons Center
ATTN: Code 240, Mr. C. J. Aronson
ATTN: Code 121, Navy Nuclear Programs Office
ATTN: Code 243, Mr. Frederick J. Gleason
ATTN: Code 242, Mr. Irving Kabik

DEPARTMENT OF THE AIR FORCE

AF Weapons Laboratory, AFSC
ATTN: SUL, Technical Library
ATTN: Mr. J. Bratton
ATTN: Robert Port

Commander
Armament Development & Test Center
ATTN: ADBRL-2

SAMSO/MN
ATTN: MNNH, MNI
ATTN: DEB

ATOMIC ENERGY COMMISSION

Sandia Laboratories
ATTN: Document Control for Dr. Walter Herrmann
2 cy ATTN: Document Control for Dr. M. L. Merritt

University of California
Lawrence Livermore Laboratory
ATTN: Douglas Stephens, L-437, Chemistry Dept.
ATTN: Jack Kahn

DEPARTMENT OF DEFENSE CONTRACTORS

Aerospace Corporation
ATTN: Dr. Prem N. Mathur
2 cy ATTN: Technical Information Services

Agabian Associates
ATTN: Dr. M. Agabian

The Boeing Company
ATTN: Dr. R. Hager

Braddock, Dunn & McDonald, Inc.
ATTN: A. Lavagnino

Civil/Nuclear Systems Corp.
ATTN: Bob Crawford

General American Transportation Corporation
General American Research Division
10 cy ATTN: Dr. G. L. Neidhardt, Manager of Engineering
ATTN: Stephen F. Fields
ATTN: Leif E. Fugelso

General Electric Company
TEMPO-Center for Advanced Studies
ATTN: DASIAC

DEPARTMENT OF DEFENSE CONTRACTORS (Continued)

Institute for Defense Analyses
ATTN: Technical Information Office

J. L. Merritt
Consulting & Special Engr Svs. Inc.
ATTN: J. L. Merritt

Kaman Sciences Corporation
ATTN: Mr. Paul A. Ellis

Nathan M. Newmark
Consulting Engineering Services
ATTN: Nathan M. Newmark

Physics International Company
ATTN: Document Control for Mr. Fred M. Sauer

DEPARTMENT OF DEFENSE CONTRACTORS (Continued)

R & D Associates
ATTN: Dr. Henry Cooper

Science Applications, Inc.
ATTN: Dr. William M. Layson

Systems, Science and Software, Inc.
ATTN: Dr. Donald R. Grine

TRW Systems Group
One Space Park
ATTN: Dr. Pravin Bhutta

Weidinger Associates, Consulting Engineers
ATTN: Melvin L. Baron